2020 ExoMars Rover landing site checklist: Aram Dorsum
M. Balme, P. Fawdon, P.M. Grindrod, J.M. Davis, S. Gupta,
17th March 2017

1. INTERESTING SCIENCE TARGETS

1.1 POSITION OF ELLIPSES

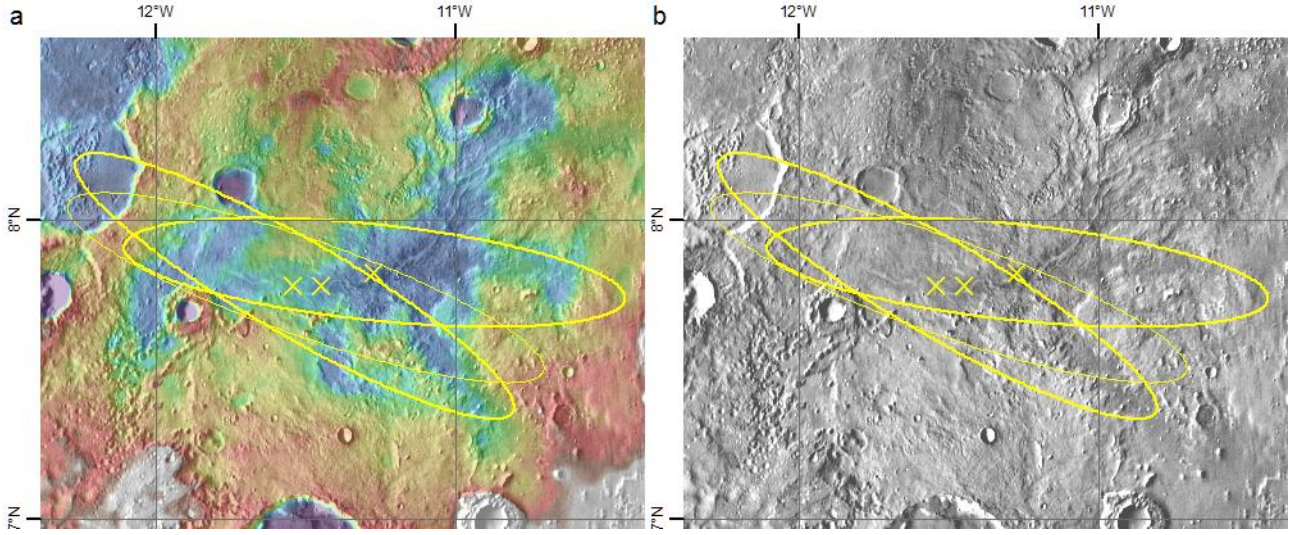

Fig. 1. *Aram Dorsum landing ellipses (max and min azimuths, 96° and 120°, and example intermediate azimuth, 109.3°) plotted against (a) MOLA topography and (b) CTX/THEMIS image.*

Table 1. *Ellipse properties at Aram Dorsum.*

Position (latitude = planetocentric)		**Azimuth**	**Dimensions (3 sigma ellipse)**	
Latitude (°N)	Longitude (°E)	(°CW from N)	Major axis (km)	Minor axis (km)
7.826163	348.729037	96	100	19
7.776191	348.497624	109.33	100	19
7.780631	348.461751	120	100	19

1.2 FIGURE OF PROBABILITY WITHIN ELLIPSES

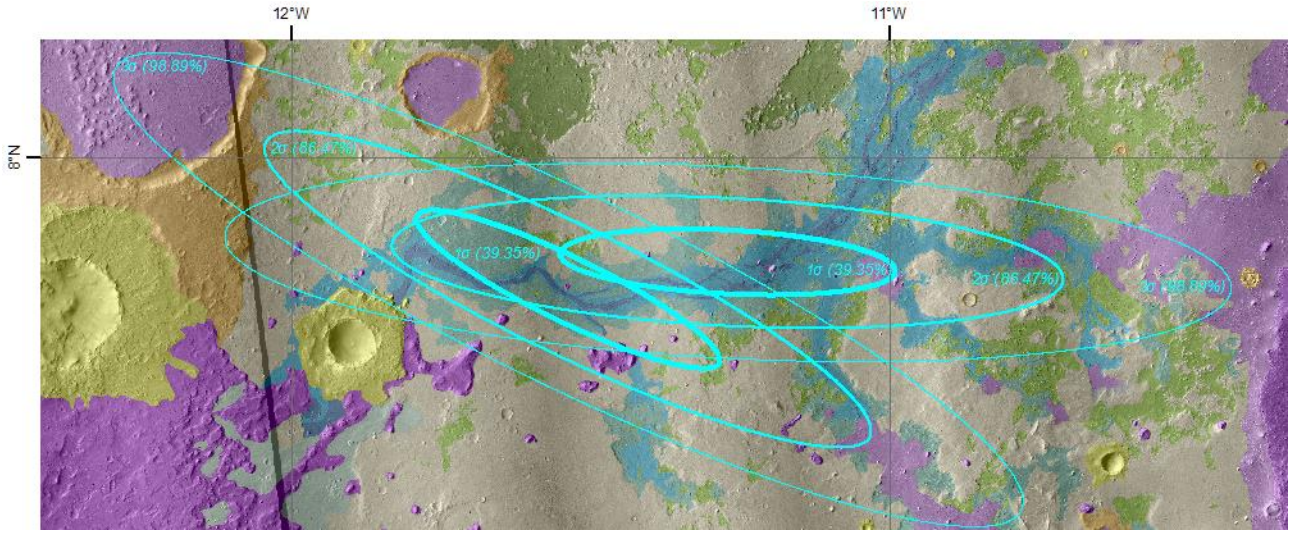

Fig. 2. *The probability of landing on high priority science targets at Aram Dorsum shown by probability ellipse at 1σ (39.35%) 2σ (86.47%) and 3σ (98.89%). These probability contours are examples derived from data provided by the LSSWG, subject to known sizing errors. For description of geological map, including science target priority, see Fig. 5.*

1.3 IDENTIFICATION OF HIGH PRIORITY TARGETS, REGIONS, AND FORMATIONS

1.3.1 Overview

Aram Dorsum is a flat-topped network of sinuous ridges set in a low relief plain in the Arabia Terra region of Mars (Fig. 3). The main ridge system of Aram Dorsum comprises a ~100 km long, ~1-2 km wide, sinuous and branching set of ridges, surrounded by extensive, low relief plains comprising layered sedimentary deposits. The ridge system is interpreted as an eroded and now inverted fluvial channel belt with the surrounding layered deposits interpreted as overbank deposits formed on former floodplains. Aram Dorsum is the type example of a much wider network of similar channel bodies[1], which formed a regional fluvial system during the late Noachian. This system potentially connected the valley networks of the southern highlands to the northern lowlands (Fig. 3a).

The overbank deposits that formed on the margins of the fluvial channel belt system are the prime target for exploration by the ExoMars Rover. These floodplain environments were likely repeatedly recharged with fine-grained sediment from an extensive upstream catchment. They provide a favourable habitable environment with the potential for the formation and concentration of biosignatures. The water-lain sediments deposited here are interpreted as fine-grained deposits, likely mudstones and very fine-grained sandstones. They are therefore key science targets for the ExoMars Rover as they have high biosignature preservation potential. These sediments also have a high probability of containing hydrous mineralogical phases, such as phyllosilicates, sulphates and hydrated silica.

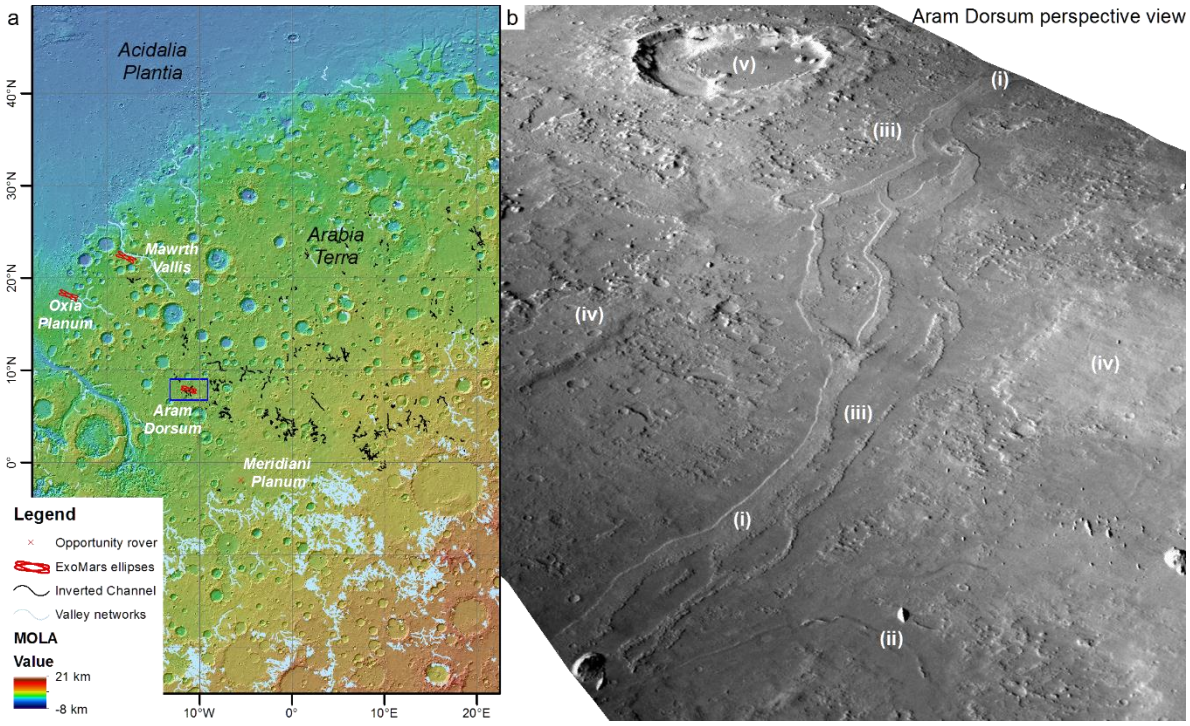

Fig. 3. *(a) Location of Aram Dorsum within Arabia Terra, in context with MER opportunity Rover and other ExoMars Rover landing sites. This shows where Aram dorsum fits in with the regional networks of valleys[2] and inverted channels. Blue box shows extent of Figs. 2 and 3. (b) Perspective view of ~ 30 km reach of the Aram Dorsum system showing (i) the main trunk of the system, (ii) a smaller tributary inverted channel (iii) smoother, flatter, plains deposits on either side of the main channel, (iv) the local overburden from beneath which the fluvial network has been exposed, and (v) craters in the early Noachian basement. Note the branching/reforming sinuous channel morphology.*

The size of Aram Dorsum, its branching shape, and the presence of a regional network of inverted channels, demonstrate that it had a large fluvial catchment. Thus, the rock record exposed here will contain sediments and possibly biosignatures that sample a range of terrains and processes

from across the wider Noachian highlands, including many possible Noachian habitable environments (ancient impact crater lakes, groundwater deposits, impact-related hydrothermal systems etc).

The channel and floodplain materials within Aram Dorsum have been exhumed from beneath regional-extent overburden materials (themselves dated to the late Noachian[3]). Thus, Aram Dorsum is at least late Noachian in age. Most importantly, Aram Dorsum has only recently (within about 30 – 200 Ma; Fig. 6) been exhumed from beneath these materials, maximising biosignature preservation potential. This is crucial for ExoMars because biosignatures deposited here will have been continuously shielded from Mars' inhospitable surface environment for 99% - 95% of the time since their deposition.

Aram Dorsum brings together: (1) an environment suitable for biosignature formation and preservations, (2) an extensive catchment region, which sampled ~1% of Mars' surface during the late Noachian, and thus maximises sample diversity; (3) a geological environment that has the potential to preserve biosignatures, and that has only been recently exhumed; and (4) access to an extensive Noachian sedimentary rock record of confidently-constrained provenance and depositional style. It is an ideal landing site to directly address questions of Mars' early climate[4] and to look for biosignatures.

Finally, the Aram Dorsum site's physiography is ideal for ExoMars Rover operations, consisting of shallow and wide pits and low ridges, with exposed layering visible in HiRISE images. Accessibility of low, vertical outcrop will be vital for mission scientists to understand the local geology and determine where to drill.

1.3.2. Palaeoenvironments, habitability and geological context

Overall, Aram Dorsum is similar in morphology and setting to many now-inverted channels systems observed on Earth (e.g., in the Cretaceous Morrison Formation in Utah USA; Fig. 4). It was once an active river system, so contained both near surface and sub-surface habitable environments. All of the fluvially-deposited sediments and possible ground-water related veins are considered targets for ExoMars, but the floodplains units are the highest priority.

a 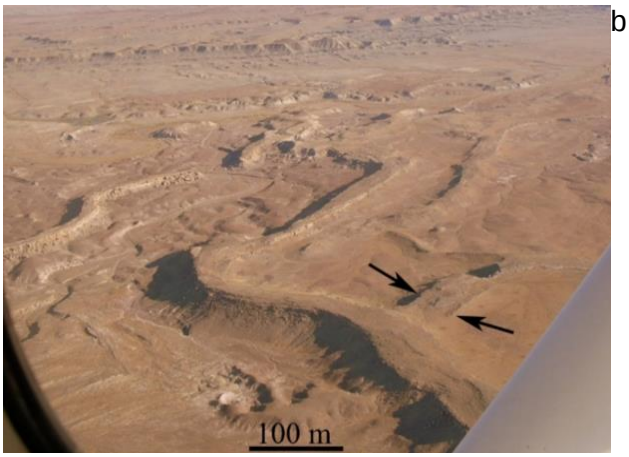

b 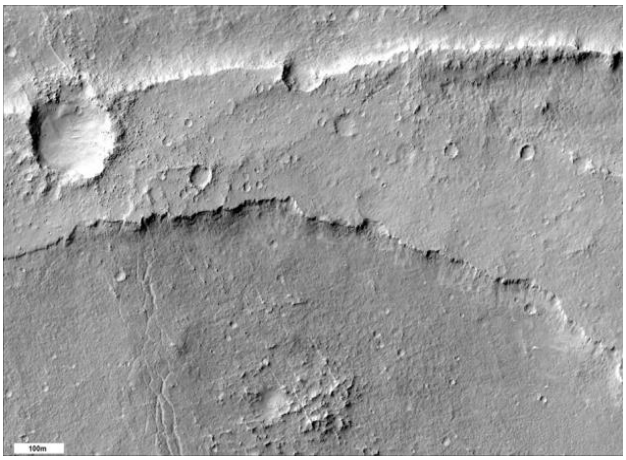

Fig 4. *(a) Inverted channel in Green River, Utah, with stacked channels providing evidence of multiple episodes of activity[5]; (b) part of the inverted channel at Aram Dorsum, with layering evident in the main channel deposits and low-relief plains surrounding it.*

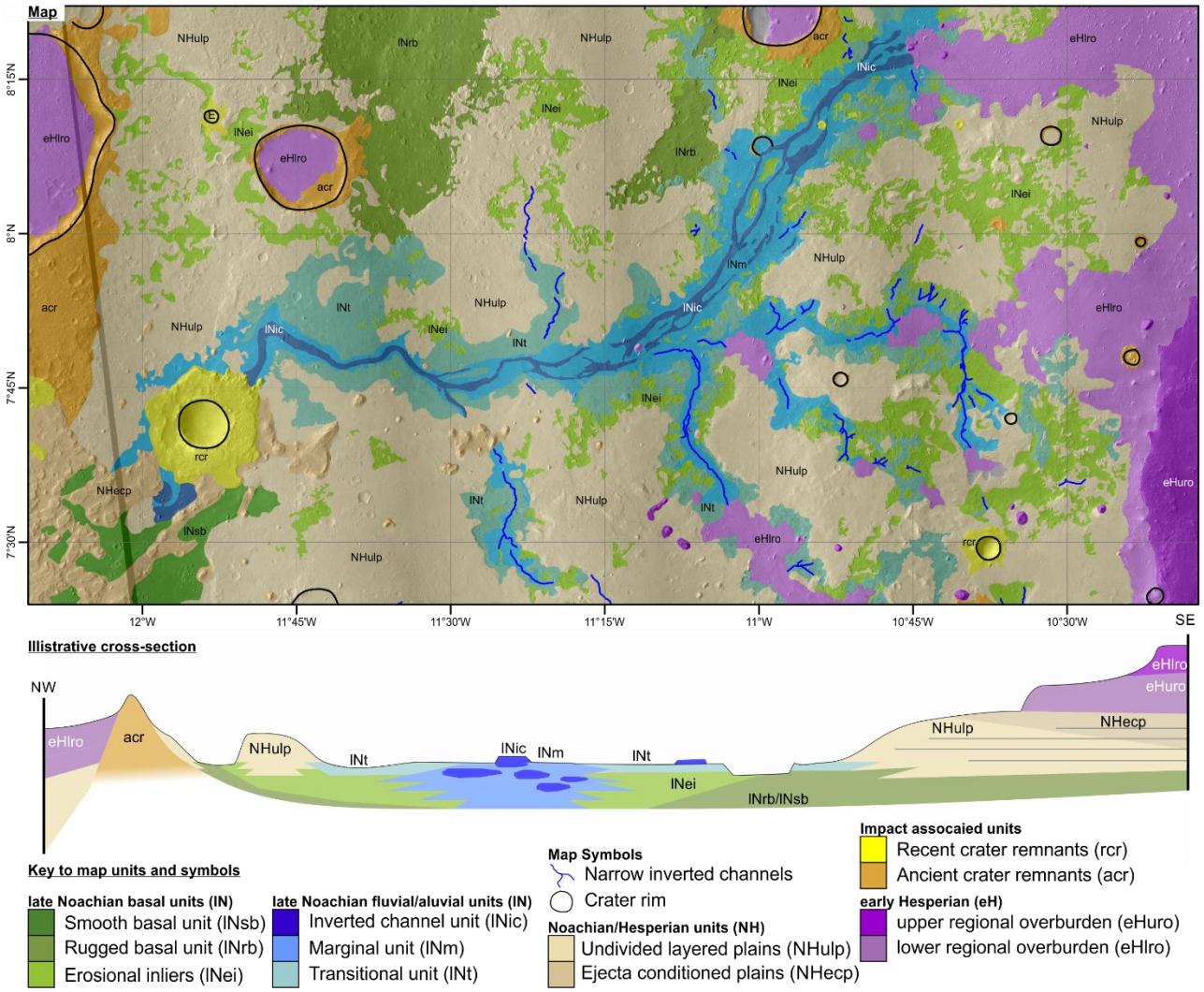

Fig 5. *Geological map of Aram Dorsum area created from CTX (6m/pixel) images. Blue areas show the late Noachian fluvial/alluvial units (inverted channels and surrounding low-lying, low relief plains) and are priority 1 science targets. Dark green areas are the late Noachian basal units, which are at a similar or lower stratigraphic level to Aram Dorsum. Mid green areas are often exposed in erosional pits, and include potentially ancient fluvial/groundwater-altered sediments (also priority 1 science targets). Dark brown and yellow areas are impact crater materials (low priority), light brown areas are what we refer to as "local overburden" materials that once buried Aram Dorsum - these are probably a combination of aeolian and fluvial sediments and ejecta from ancient impacts. Thus, they could also contain biosignatures (medium priority). Pink areas are the eroded remains of mid/late Noachian regional "etched units" (or "regional overburden units") that once covered the entire area. They are thought to be pyroclastic deposits of low priority for ExoMars Rover.*

Age - Noachian

Aram Dorsum lies in the Late Noachian highland unit on the global geological map[6] and in the Noachian Meridiani Etched One (NMe_1) unit in the regional geological map of Greater Meridiani Planum[3]. While impact crater size/frequency statistic-based ages determined at these scales (1:20M Global, 1:2M Regional) are not truly applicable to the high resolution stratigraphy of the landing ellipse, local stratigraphic relationships (Fig. 5) indicate that Aram Dorsum is clearly beneath and therefore older than these regional units. Where we have collected impact crater size-frequency statistic, the data support this conclusion: the Aram Dorsum system is at least late Noachian (> 3.7 Ga) in age, possibly older.

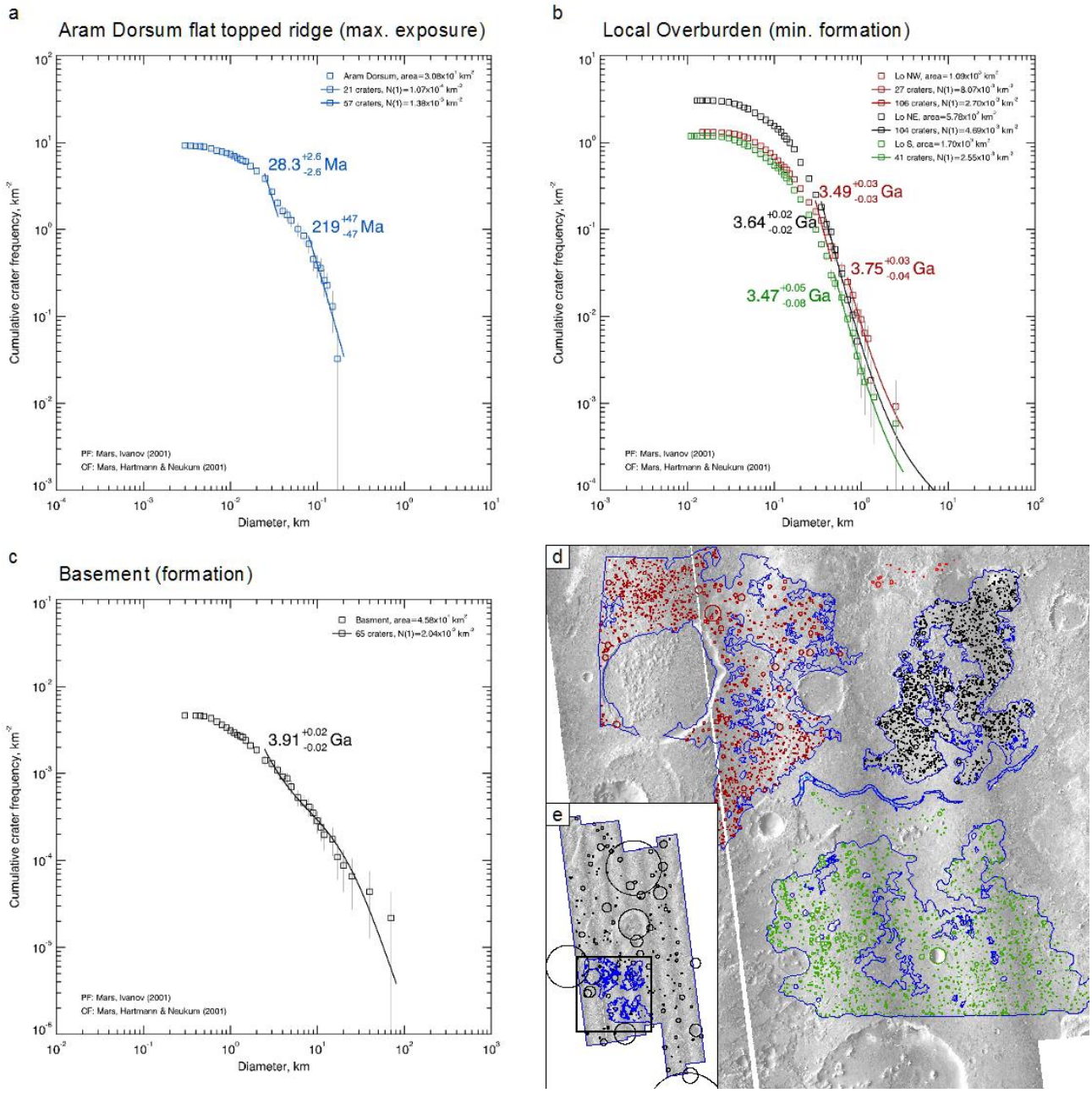

Fig. 6. *Crater counting age estimates at Aram Dorsum. (a) Exposure ages of the Aram Dorsum main channel belt, (b) crater retention ages of local overburden ages, giving a minimum age for Aram Dorsum, (c) crater retention age of basement material, (d) crater count areas.*

Fluvial Channel-belt system

The main geomorphic feature at the Aram Dorsum landing site is a ~100 km long, 1-2 km wide, sinuous and branching, flat-topped ridge. The ridge trends roughly north-east to south-west and is bound by low-relief plains. The presence of metre-scale layering within the ridge margins support a sedimentary origin. The main ridge comprises multi-thread segments with distinct anabranching geometries. Thus, the ridge at Aram Dorsum is interpreted as an exhumed fluvial channel system. It is surrounded by low-relief plains, which are mainly superposed by the channel units, but on occasions themselves bury traces of former channels. We therefore interpret these as floodplains deposits, similar to numerous inverted systems elsewhere in martian[5] and terrestrial[7] settings.

In contrast to the martian valley networks, inverted channels do not incise into bedrock. Instead, they form in an aggrading, alluvial landscape, and the channel fill and lateral plains materials are composed of transported fluvial sediment. Chemical cementation or the deposition of

coarse material within the channel leaves the channel-body resistant to erosion. The channel body then becomes exhumed due to preferential erosion of surrounding floodplain deposits, leaving the channel body upstanding in the landscape.

The scale and complex morphology of Aram Dorsum suggest it was a long lived system and not formed by single event. Contributory channels to the main channel indicate that Aram Dorsum was once part of a larger system with a distributed source of water (i.e., regional precipitation). The interbedding of channel material with the adjacent low-relief deposits supports[8] the interpretation of Aram Dorsum as an aggrading alluvial system.

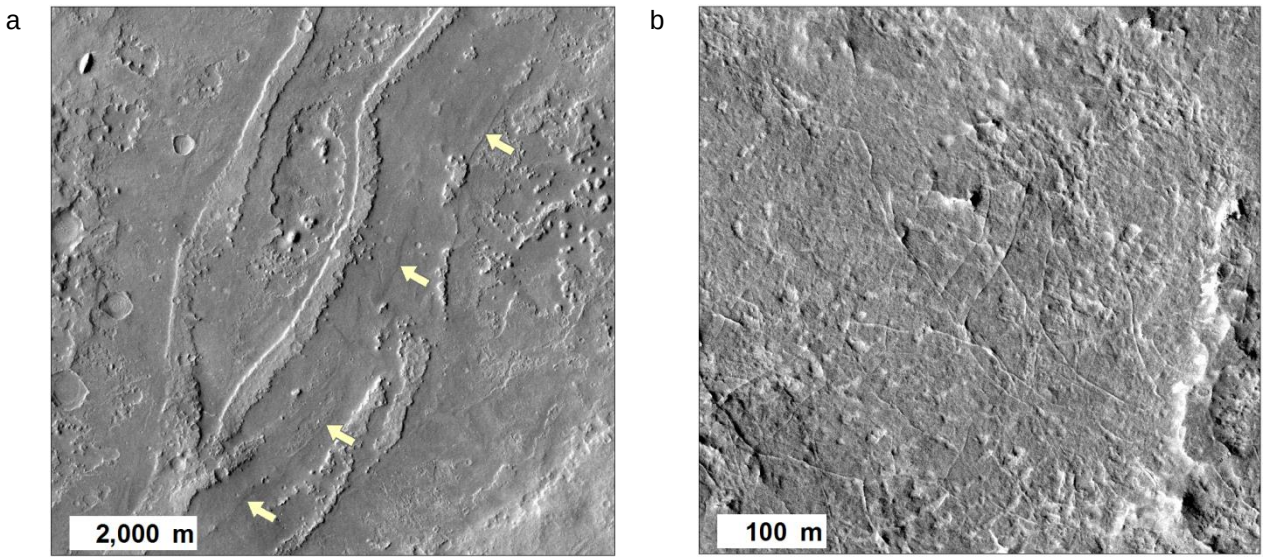

Fig. 7. *Example morphologies in Aram Dorsum. a) Buried channel segments (arrowed) within low-relief channel margin (floodplains) deposits. b) Example of small vein-like landforms of possible groundwater origin. These are seen within erosional pits in and near the channel margin deposits and always occur near the bottom of the local stratigraphy.*

Floodplain deposits

The Aram Dorsum inverted channels are surrounded by distinct, low-relief plains (Fig. 5) comprised of layered (i.e. almost certainly sedimentary) rocks, from which the inverted channel bodies are eroding. These plains are best interpreted as exhumed floodplain deposits, consisting of fine-grained sediments that were deposited as the Noachian landscape aggraded, and are now likely lithified to mudstones and very fine-grained sandstones.

Within the floodplain layered units a variety of structures are observed in HiRISE images which have implications for reconstructing the palaeoenvironment. Decametre-scale polygonal fractures are present within the uppermost floodplain units, with wider, shallow polygonal troughs in the lower floodplain material, exposed in numerous shallow erosional depressions. We cannot determine the origin of these features, but they correspond spatially with the channel marginal unit. They could be sub-aerially formed structures (due to desiccation of wet sediment or thermal contraction of ice-rich sediment), or they could be sub-surface features such as joints, formed during burial and unloading. Similarly patterned deposits are found adjacent to many other inverted channelbelt systems in Arabia Terra, and have been shown to contain phyllosilicate minerals in at least one case (see section 1.3.3). In addition, “vein-like” curvilinear ridges, <1 m wide and tens of metres long, are found in the stratigraphically lowest erosional pits in areas close to the channel deposits. These features could be groundwater related mineralised veins or fracture fills.

The floodplain deposits adjacent to the channelbelt systems are the highest priority ExoMars Rover science targets and the most extensive sedimentary deposits in the centre of the landing ellipse. The sediments deposited here likely comprise high concentrations of very fine-grained

sandstones and mudstones, derived from Aram Dorsum's extensive catchment area. These materials are likely to have a good biosignature preservation potential[9], due to rapid burial during channel flooding and overbank sedimentation, which will ensure any biosignatures are protected from oxidising surface conditions[10].

Regional Catchment

Aram Dorsum is the "type example" for the Noachian inverted channelbelt systems found across Arabia Terra[1], and is representative of the Noachian regional alluvial sediment routing systems that were sourced from extensive catchments. A first order estimate of the Aram Dorsum catchment area can made by estimating paleodischarge based on the channel width[11]. For Aram Dorsum, with ~1-2 km width, the paleodischarge estimate is 10^4 - 10^5 m^3s^{-1}. This can then be used to further estimate the catchment area[11], which for Aram Dorsum is ~1.4 x 10^6 km^2. This is equivalent to ~1% of Mars' surface, or the area of north-west Europe.

The large catchment includes the Noachian highland valley networks, and therefore samples diverse and scientifically important terrains such as impact-induced hydrothermal bedrock, palaeolake sedimentary units, and ancient igneous terrains. It is plausible that biosignatures may have formed within (or been funnelled into) these catchments and then transported and deposited in the Aram Dorsum depositional system, forming allochthonous biosignatures. A large regional catchment increases the diversity of the source materials supplied to the depositional system, providing a window into the broad chemistry of martian bedrock terrains.

Furthermore, Aram Dorsum's position within the regional Arabia Terra alluvial plain, reinforces its stratigraphic association with large Noachian terrains, the late Noachian valley networks, and areas of phyllosilicate outcrops. Significantly, MSL has shown good evidence for habitability at Gale Crater during the early Hesperian[12], but no obvious examples of biosignatures. Consequently, Hesperian-aged fluvial systems and their deposits (such as Coogoon Vallis at Oxia Planum) may not fulfil the ExoMars Rover mission objectives. Aram Dorsum thus presents a unique opportunity to sample a late Noachian alluvial system that was supplied by a large and diverse regional Noachian catchment.

Burial - preservation – exposure

At the periphery of the landing ellipse, the Aram Dorsum inverted channels and associated floodplain deposits are buried by local and regional overburden deposits. Local outliers of overburden are found in the southern part of the landing ellipse, exposed as smaller buttes, which indicate that the underlying alluvial stratigraphy were once entirely buried before recently being exhumed. These stratigraphic relationships have two important implications for the ExoMars mission goals. Firstly, these overburden materials form an ~800 m thick regional stratigraphy, a stack of units which extends from Aram Dorsum (deposited in the late Noachian) to Meridiani Planum (deposited in early Hesperian)[13]. Thus Aram Dorsum site must be older than these units and has been buried since at least the Noachian/Hesperian boundary and has only recently been exhumed. Secondly, the small steep buttes and lack of impact craters on the inverted channel and marginal plains indicate that the site is being actively exhumed today. Actively eroding scarps and erosional windows are considered ideal sample sites for finding well-preserved biosignatures[14].

Summary

Geomorphic observations indicate that Aram Dorsum is an exhumed, inverted former river channel belt. It was deposited by a large river system fed by a large drainage basin in the late Noachian. The 100-km scale preserved length of the channel belt strongly indicates that it was fed by sustained fluvial discharges. The sedimentary units forming the plains regions adjacent to the inverted channel represent overbank deposits formed by decanting of water and sediment from the

fluvial channels onto floodplains. These overbank environments that may have comprised sub-environments of lakes, ponds and floodplains and likely provided extensive habitable environments on early Mars that were conducive to the preservation of both in situ microbial life and transported biosignatures if they had existed. The Aram Dorsum site was rapidly buried at the Noachian/Hesperian boundary and was only recently exhumed, increasing the preservation potential of biosignatures. All of the fluvial and alluvial sediment, as well as possible groundwater related features, are considered high priority science targets for ExoMars. Crucially for the ExoMars mission, the understanding of the geological context, the extensive catchment providing a wide diversity of sediment sources, and recent exhumation of the site will maximise the likely fulfilment of the science goals within the limited timeframe of the mission.

Importantly, Aram Dorsum now has a well understood geological context, which is conducive to Rover exploration. It will be possible to test hypotheses using the Rover's remote sensing suite (PanCam, HRC, ISEM), minimising the time developing context science. Both unit surfaces and lateral outcrops of the inverted channel are accessible, as are those of the floodplains units (via shallow depressions and flat-bottomed pits). Hence WISDOM can be used to characterise the 3D sedimentary architecture from above, with side-views of outcrop being used to better understand the geological setting. This compares favourably to both Oxia Planum, where the lack of geomorphic relief is not conducive to establishing stratigraphy without considerable driving distances, and Mawrth Vallis, where drilling into exposed stratigraphy is inhibited by steep scarps and the presence of basaltic composition capping units.

1.3.3 Mineralogy of Aram Dorsum

The presence of a thin dust cover (likely of the order of microns thick) in the Aram, and wider Arabia Terra region, precludes most direct identifications of hydrated mineralogies from current orbital spectrometers. However, the presence of hydrated and hydrous minerals can be confidently inferred in Aram Dorsum using several lines of evidence.

1. Dust-free windows and phyllosilicates. Much of Mars is dominated by nanophase ferric oxide (NFO) signatures. Hence, it can be difficult to tell what minerals are present beneath this <100 μm thick 'dust' cover[15]. However, in the wider Aram Dorsum region, there are "dust-free" windows that allow the underlying mineralogy to be determined from orbit. OMEGA data reveal the presence of Fe/Mg and Al phyllosilicates in terrains similar in stratigraphic position and morphology to those in the landing ellipse (Fig. 8). There are also possible sulphates in a southern crater rim[16].

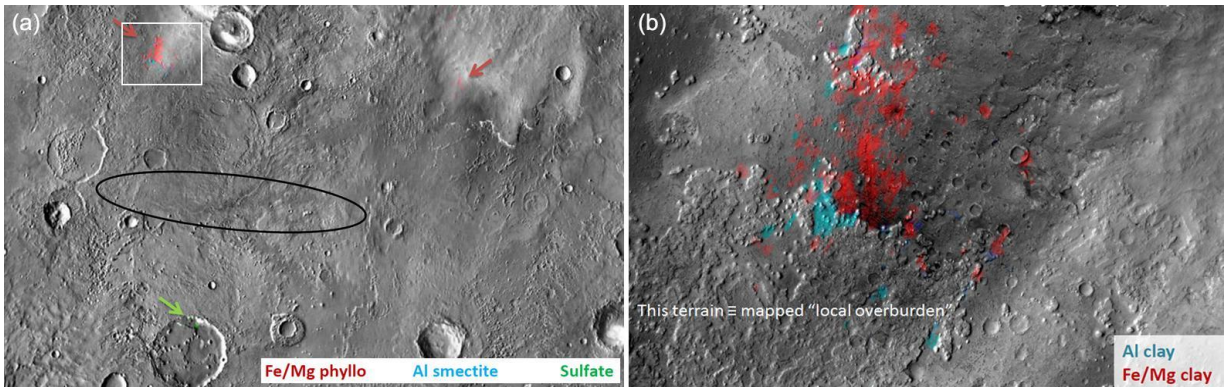

Fig. 8. *Phyllosilicates in dust-free windows at Aram Dorsum. (a) Example ellipse for Aram Dorsum and location of phyllosilicate and sulfate deposits. White box shows location of (b), which shows a "Mawrth-type" stratigraphy of Fe/Mg phyllosilicates underlying Al phyllosilicates, in material the same as the units mapped in the Aram Dorsum ellipse. Images courtesy of John Carter.*

2. Inverted Channel in Miyamoto Crater (Fig. 9). The type mineralogy at inverted channels can be seen at Miyamoto Crater, SSE of Aram Dorsum. Here, Fe/Mg phyllosilicates occur in terrain either

side of the channel capping layer[17]. The hydrated deposits are found in a polygonally fractured terrain is interpreted to have formed/been modified by aqueous processes, although an allochthounous or autochthonous origin cannot be determined at Miyamoto[17]. The Aram Dorsum channel marginal material contains the same polygonised texture in the same location relative to the channel. Other examples of Fe/Mg phyllosilicates associated with inverted channels occur (e.g. ~10.5°N, 5°W), suggesting inverted channels contain at least some of the same mineral stratigraphies found at Oxia and Mawrth, and are representative of the wider Arabia region[18].

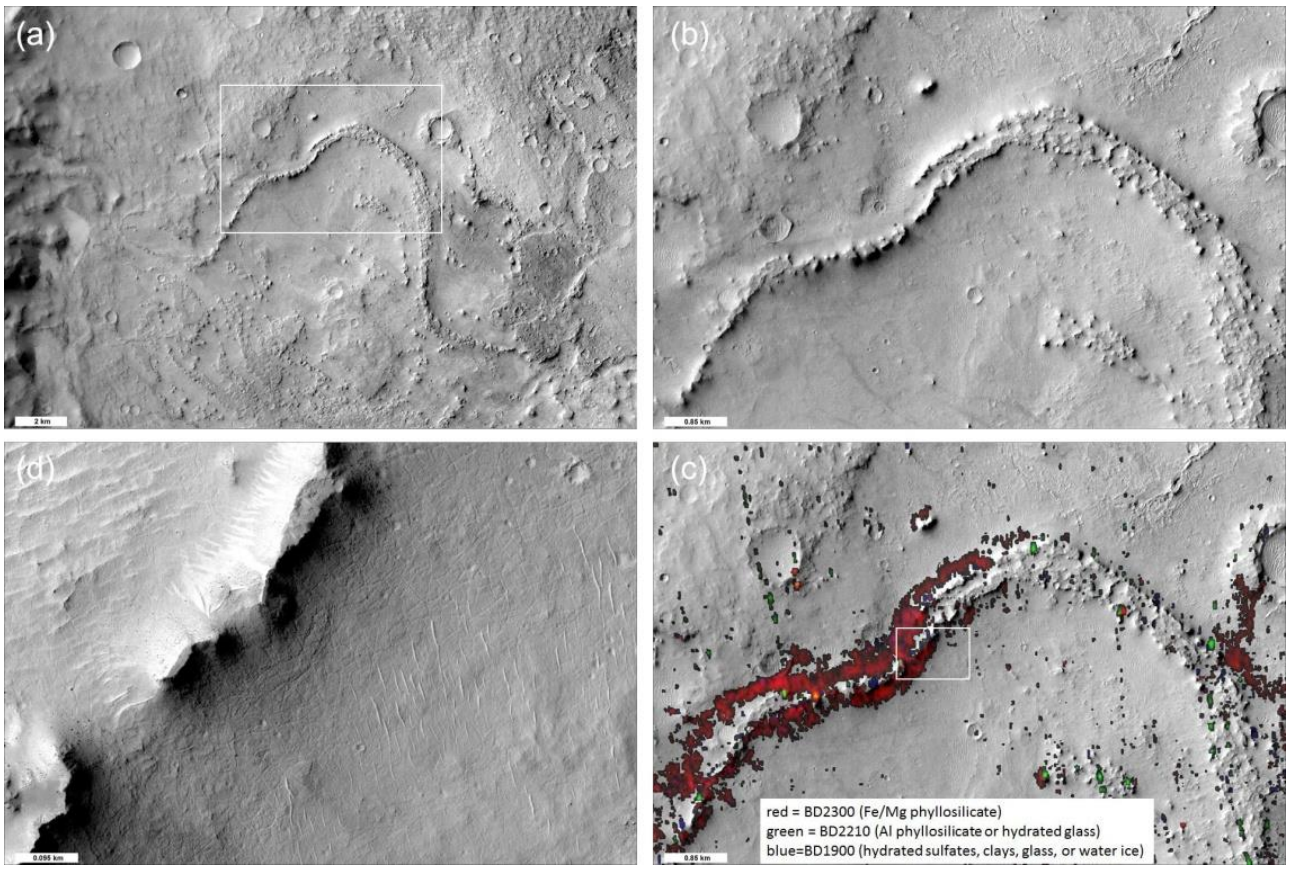

Fig. 9. *Phyllosilicates at an inverted channel at Miyamoto Crater. (a) CTX context image of the inverted channel, showing location of (b) a close-up view of the inverted channel. (c) Same image as (b), but with CRISM phyllosilicate parameter image overlaid, and showing location of (d) polygonised terrain associated with the phyllosilicates.*

3. Analogy with MSL Yellowknife Bay drill sites. The presence of a diverse hydrated mineralogy and evidence of a habitable environment was discovered by MSL at a landing site with no previous supporting orbital evidence at that location[12]. Detailed XRD analysis of the John Klein and Cumberland mudstones by the CheMin instrument on MSL has revealed the presence of ~20 wt.% smectite, and ~5 wt.% hydrated and anhydrous sulfates[19]. Although suggested by CRISM data in Aeolis Mons prior to site selection[20], no aqueous mineralogy has been observed at the Yellowknife Bay site with CRISM data[21].

1.4 Probability of Reaching High Priority Targets

High priority targets are defined for Aram as being part of the Aram Dorsum fluvial units group, or being the polygonized areas exposed within erosional pits (i.e. layered terrains that appear to be related to the Aram Dorsum floodplains). These are generally in the centre of the ellipse pattern. We defined 1, 3 and 5km buffers from the locations of these areas (Fig. 10). The majority of the ellipse is within the 1km buffer, and this is especially the case for the 1σ and 2σ ellipses. Almost all

of the 1-3σ ellipses are within the 3km buffer, with the exception of the westernmost ends of the high azimuth ellipses. We conclude that there is a high probability of landing directly on science targets, and a very high probability of landing within 1 km.

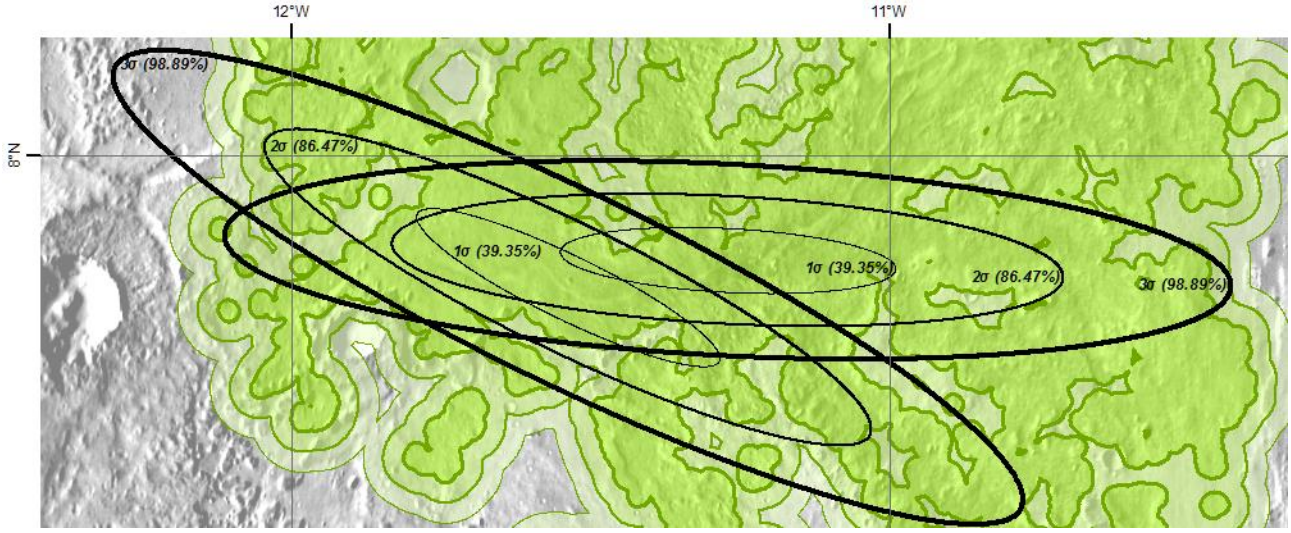

Fig. 10. *Example Aram Dorsum* 1-3σ *ellipses (max and min azimuth) with 1 km (dark green), 3 km (mid-green) and 5 km (pale green) buffers constructed from primary science target locations.*

2. TERRAIN AND HAZARDS

2.1 INTRODUCTION AND METHOD

We produced elevations and slope maps for the whole range of baselines detailed in the 2013 call for landing site proposals[22] for all three sites. We also produced impact crater distribution and aeolian hazards (Transverse Aeolian Ridges) distribution maps for all three sites. These data are included for completeness in the attached appendix, with mainly Aram-specific data shown here.

In most areas we used several methods for quantitative analyses. For example, we used MOLA (gridded and point), HRSC and CTX for elevation data, and used two different methods ('sl' and 'mas'; described in appendix) for the slope maps. Where possible we have used data that cover the entire ellipse pattern. Where such data are not available, we used all available data in the ellipse pattern. Data availability for all three sites is shown in appendix.

For elevation and long baseline slopes (where data coverage covers all/most of the landing ellipse patterns) we have studied 10 ellipses, with azimuths equally spaced across the full azimuths range provided by the LSSWG. This allows us to explore the full range of potential azimuths within the launch window. For short baseline slope data (i.e. evaluated using HiRISE DTM's) we initially sampled 'per DTM'. However, this does not sufficiently explore the spatial variations in the data. Therefore, we have sampled the HiRISE data using a 1x1 km grid, giving a better exploration of the areas of good and bad slopes.

2.2. Elevation and Slope hazards

These data are split into (i) elevation and long baseline slopes (calculated for the whole ellipse) and (ii) short baseline slopes (calculated only where HiRISE DTMs exist). Figure 11 summarises the spatial variation of elevation and long baseline slope hazards.

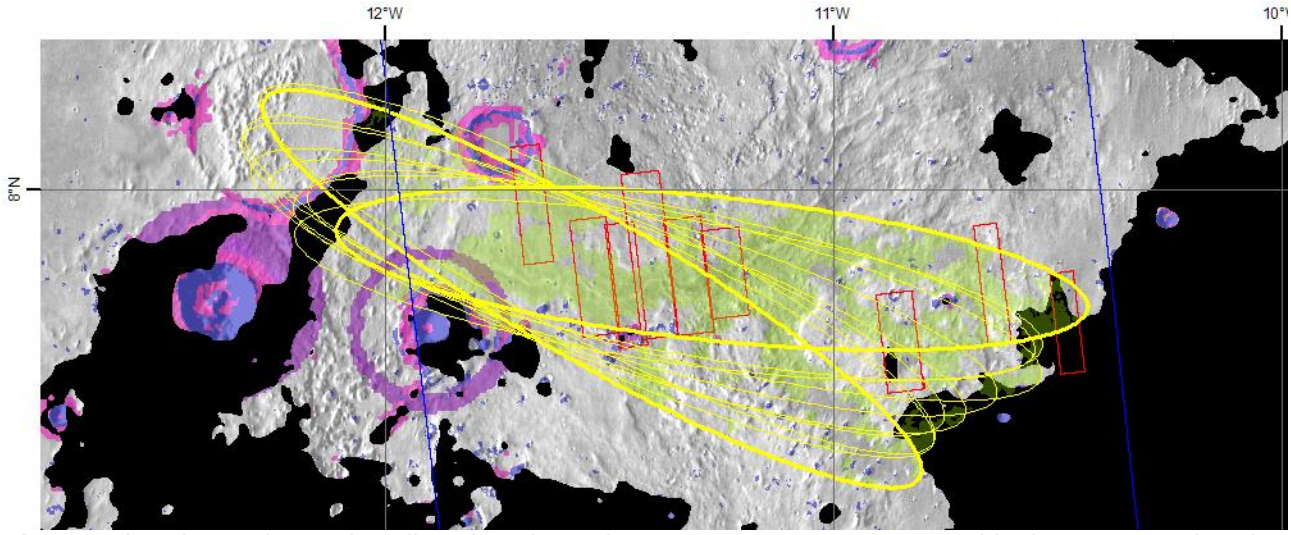

Fig. 11. *Elevation and Long baseline slope hazards at Aram Dorsum. Areas outside the -2000 m elevation criterion are shaded* ***black****. Areas that exceed the various slope criteria (calculated by both methods) are coloured by baseline: 10 km in* ***purple****, 2 km in* ***pink*** *and 330 m in* ***blue****. The thick yellow ellipses show the maximum and minimum azimuth ellipses and the lighter yellow ellipses denote the 10 sample azimuths used to evaluate the elevation and long baseline slope hazards. Pale green shading shows areas of highest science priority. Coverage of HiRISE DTM's is shown in red outlines, and CTX DEMs in blue outlines.*

2.2.1 Elevation

We have used HRSC and MOLA data to compare the elevation constraints (i.e., terrain must be < -2000 m) at Aram Dorsum with that of Oxia Planum and Mawrth Vallis. For each site, we used the same method of sampling 10 ellipses with azimuths spread equally across the range of the 2020 launch window. We used a variety of ellipse centre points to minimise violations of these engineering criteria and maximise landing on the highest priority science targets. For Mawrth Vallis and Oxia Planum, these centre points were selected with (or by) the relevant proposers. Figure 12 summarises these data.

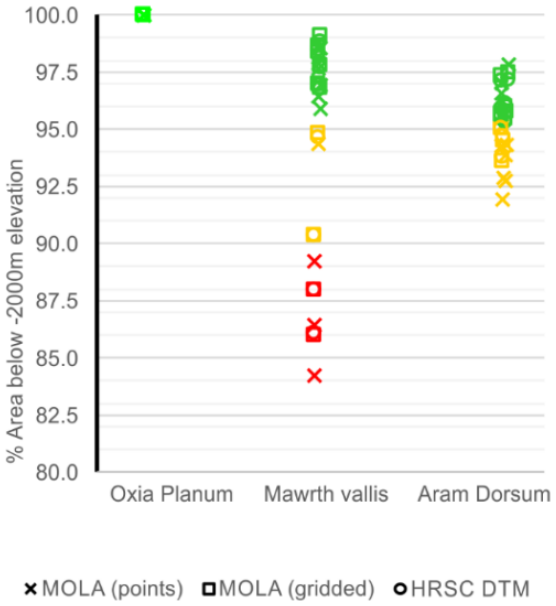

Fig. 12. *The percentage area below the -2000m elevation criteria for 10 azimuths at each of the proposed landing sites. Point shape shows dataset used; colours indicate percentage of that ellipse that passes the -2000 m criterion (green > 95%; yellow 90-95%; red <90%).*

Elevation Summary

- Across the Aram Dorsum landing ellipse pattern, areas exceeding the -2000 m criterion are limited to the far eastern end of the landing ellipse and a narrow band in the far west.
- Aram Dorsum does not meet elevations constraints as well as Oxia Planum but performs well compared to Mawrth Vallis, where >10% of the landing ellipse is above -2000 m for high azimuths ellipses. This could be migrated for Mawrth Vallis by shifting ellipse centres, making it comparable to Aram Dorsum. However, this would reduce access to targets and increase the violations of the 10km and 2 km slope criteria.

2.2.2 *Long Baseline Slopes*

Slopes over long baselines (2 km to 10 km, and 330 m) are important to ensure that slant and incidence are compatible with the radar system and that there is proper fuel consumption during powered descent. Again we sample 10 ellipses across the expected range, with the same centre points as per section 2.2.1, and use two different slope algorithms (see Appendix) to assess what percentage of each ellipse fails the criteria. Summary data are shown in figure 13 and Table 1.

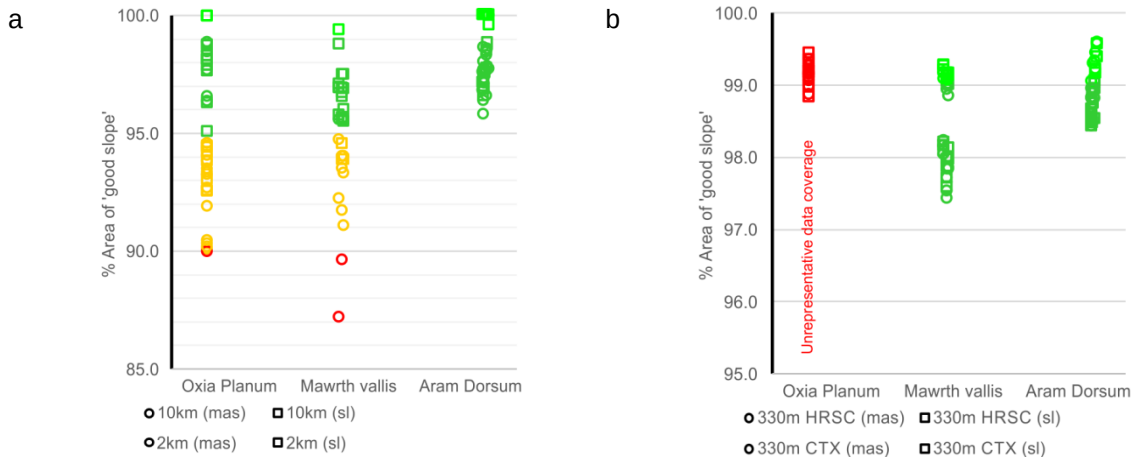

Fig. 13. *The percentage of 'good' long baseline slope areas for each site. (a) 2 km (criterion: <2˚) and 10 km (criterion: <3˚) baselines. (b) 330 m baseline (criterion: < 8.6˚). Both the 'sl' and 'mas' method results are shown, differentiated by point shape. 2 and 10 km baselines use MOLA data; 330 m baseline data shown are for both HRSC and CTX data. Note incomplete CTX DEM coverage for Oxia Planum (see appendix). Colours as Fig. 12.*

Table 1. *Long baseline statistics for 10 sample azimuths at all landing sites. Percentage given shows the area that meets the criteria; high is good, low is bad.*

Baseline/Landing site	***Mean (%)***	***Max (%)***	***Min (%)***	***Stan dev***
Baseline 10 km (2˚)				
Aram Dorsum	*98.8*	*100.0*	*96.6*	*1.3*
Mawrth Vallis	*88.9*	*99.4*	*76.1*	*8.3*
Oxia Planum	*91.8*	*100.0*	*89.9*	*3.6*
Baseline 2 km (3˚)				
Aram Dorsum	*97.6*	*100.0*	*95.8*	*1.1*
Mawrth Vallis	*94.6*	*97.1*	*89.6*	*2.1*
Oxia Planum	*96.0*	*98.9*	*92.5*	*2.4*
Baseline 330 m (8.6˚)				
Aram Dorsum	*98.9*	*99.6*	*98.4*	*0.4*
Mawrth Vallis	*98.5*	*99.3*	*97.4*	*0.6*
Oxia Planum	*99.1*	*99.4*	*98.8*	*0.2*

Long baseline slope summary

- At Aram Dorsum there is only minimal (<5%) infringement of the 2-10 km baseline criteria associated with gentle scarps of degraded crater rims at the northwest, southeast and far eastern end of the ellipse pattern. For the 330 m baseline, poorer areas follow the same pattern with a minimal addition from small mesas south of the ellipse central regions.
- At a 2-10 km baseline, Aram Dorsum has more areas that meet the slope safety criteria than either of the other sites. At Oxia Planum, craters to the east compromise all ellipse azimuths. In Mawrth Vallis, steep slopes to the north and a crater rim to the north east compromise all azimuth ellipses. At these baselines, Aram appears to be the safest site (see Appendix).

- At a 330 m baseline, all sites perform well with the data available (note that at Oxia Planum CTX DEM cover excludes the large crater at the eastern end of the ellipse pattern). The infringements of the criteria at Oxia Planum and Aram Dorsum are localised, but at Mawrth Vallis steep slopes associated with impact craters and small areas of capping unit scarp slopes are distributed across the ellipse.

2.2.3 Short Baseline Slopes (by DTM)

To evaluate slopes over short baselines (i.e. evaluated using HiRISE DTM data) we first evaluated the data on a per HiRISE DTM basis. This was done because HiRISE DTM coverage is generally in the centre of the ellipse (e.g. Fig. 11) and so is representative for all azimuths. Figure 14 and table 2 summarise these data for each site at both the 7 m (12.5˚ slope criterion) and 2m (15˚ slope criterion) baselines.

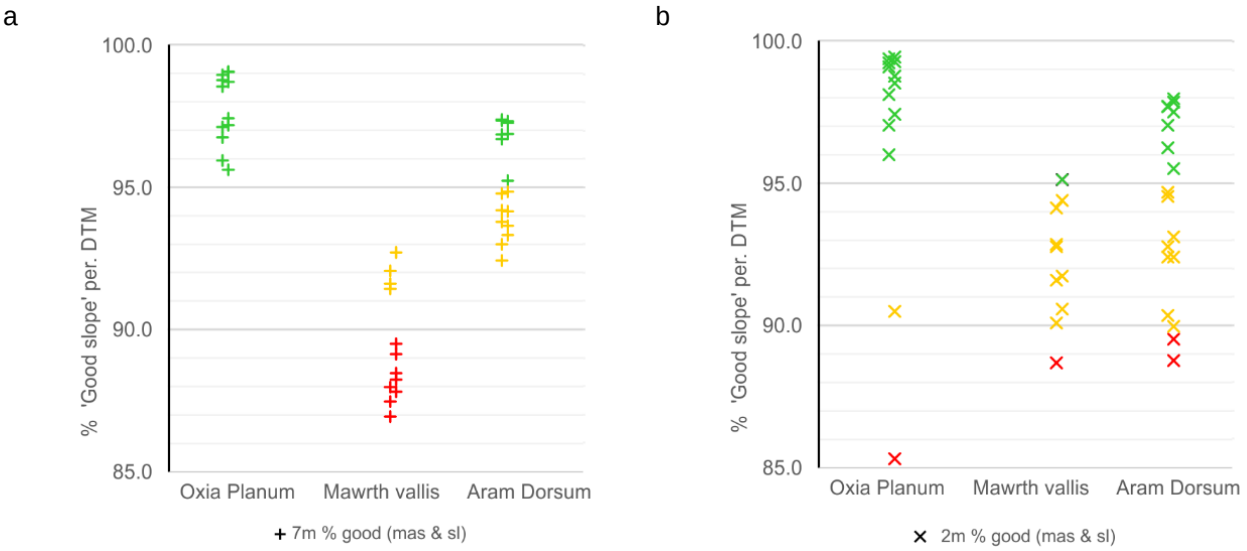

Fig. 14. *Per DTM Short baseline slope summary. The percentage of 'good' areas per HiRISE DTM is shown for the (a, left) 7 m (12.5˚) and (b, right) 2 m (15˚) baselines for DTM's in each of the three landing ellipse patterns. The results include both the sl and mas method. DTMs with poor quality data (e.g. "Oxia 3 and 6") have been removed.*

Table 2. *Short baseline slope criteria statistics for all landing sites (per DTM basis). Percentages given show the fractional area that meets the criteria; high is good, low is bad.*

Baseline/Landing site	Mean (%)	Max (%)	Min (%)	Standard deviation	no. DTM's sampled
Baseline 7 m (12.5˚)					
Aram Dorsum	*95.4*	*97.2*	*92.4*	*1.7*	*16*
Mawrth Vallis	*89.4*	*92.7*	*87.0*	*2.0*	*12*
Oxia Planum	*95.4*	*89.9*	*80.6*	*5.9*	*14*
Baseline 2 m (15˚)					
Aram Dorsum	*94.2*	*97.9*	*88.8*	*3.0*	*16*
Mawrth Vallis	*90.6*	*95.1*	*82.2*	*4.1*	*12*
Oxia Planum	*95.7*	*98.9*	*83.3*	*5.4*	*14*

2.2.4 Short Baseline Slopes (by 1x1 km samples)

We gridded the HiRISE DTMs because sampling by a full HiRISE DTM area poorly explores the distribution of slopes across the ellipse and does not cover the full area of the ellipse. This method better summarises the range of slopes seen across the various sites and ellipse options. The data are shown in Figure 15 and table 3.

Aram Dorsum

a) *7 m Baseline*

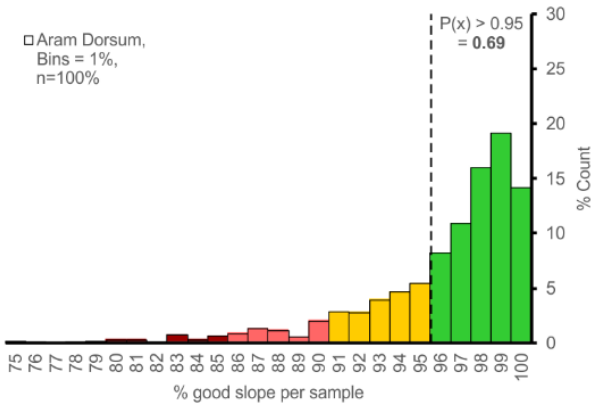

b) *2 m Baseline*

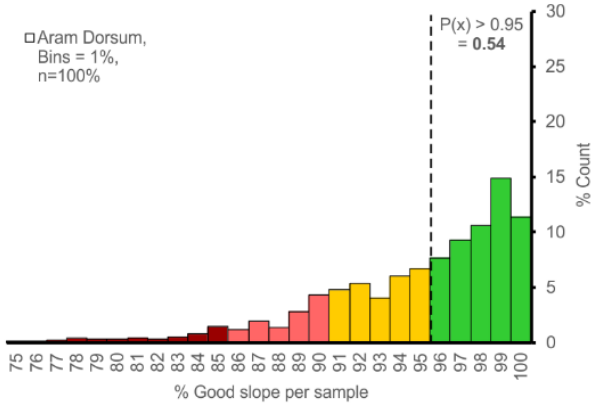

Mawrth Vallis

c) *7 m Baseline*

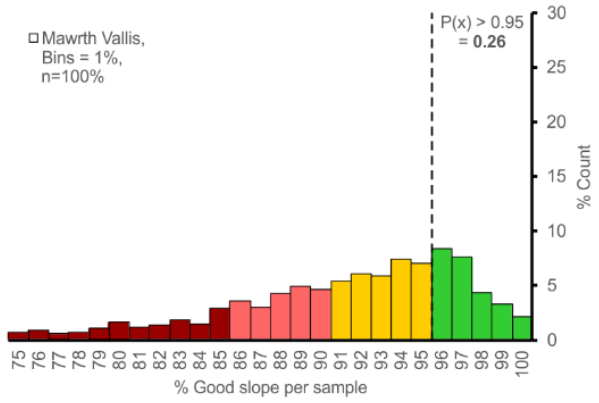

d) *2 m Baseline*

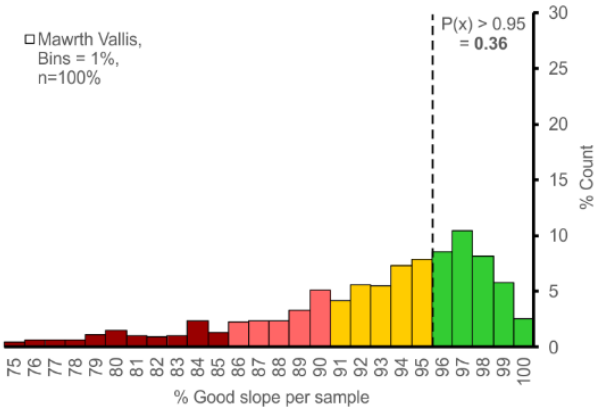

Oxia Planum

e) *7 m Baseline*

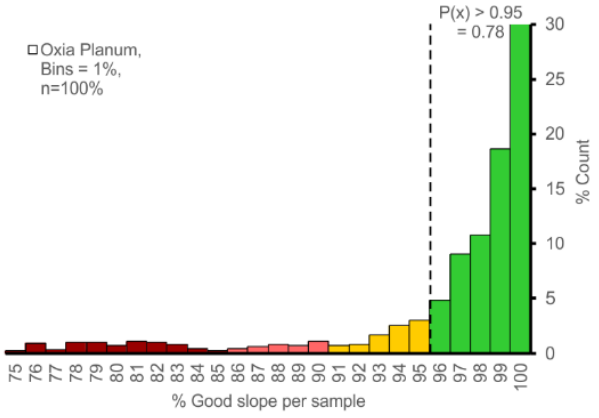

f) *2 m Baseline*

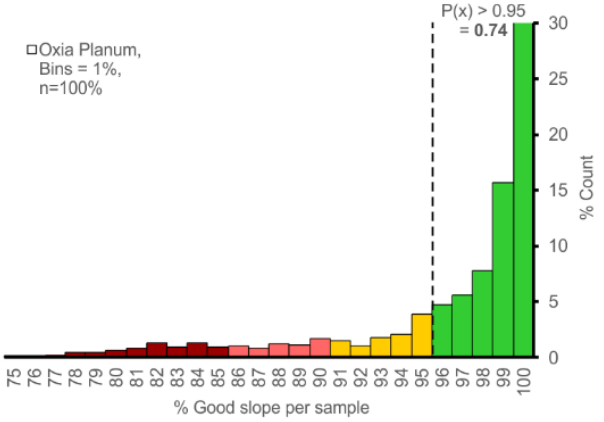

Fig. 15. *HiRISE DTM gridded short baseline slope summary. The percentage of each 1x1km DTM grid that met the slope constraints was determined using both sl and mas methods. The results are shown in the form of histograms that display the distributions of good and bad grids per site. "Safer" sites have data clustered to the right of the histogram in green; "riskier" sites have substantial higher numbers of low good-percentage cells shown in red and orange.*

Table 3. *Short baseline slope criteria statistics for all landing sites (per 1x1 km grid basis). Percentages given show the fractional area that meets the criteria; high is good, low is bad. "P(x)>0.95" shows the amount of grids with more than 95% of their area passing the slope criteria.*

Baseline	***Mean %***	***Max %***	***Min %***	***Stan dev***	***P(x) > 0.95***
Aram Dorsum					
7 m (12.5˚)	*94.6*	*100.0*	*27.0*	*7.5*	*0.69*
2 m (15˚)	*93.6*	*100.0*	*36.7*	*6.7*	*0.54*
Mawrth Vallis					
7 m (12.5˚)	*88.0*	*100.0*	*26.2*	*9.4*	*0.26*
2 m (15˚)	*90.0*	*100.0*	*17.6*	*7.0*	*0.36*
Oxia Planum					
7 m (12.5˚)	*95.3*	*100.0*	*22.8*	*8.0*	*0.78*
2 m (15˚)	*95.0*	*100.0*	*38.3*	*7.0*	*0.74*

Short baseline slope summary

- At Aram Dorsum there is only minimal (<5%) infringement of the 7m baseline criterion. Violation of this criterion are found at the degraded crater rims and isolated mesas described previously and towards the edge of the landing ellipse in the overburden terrains.
- At Aram Dorsum 69% of 1x1 km samples have <5% violation of the 7m baseline criterion. This is comparable to Oxia Planum (78%) but substantially better than Mawrth Vallis (only 26%), where steep scarps associated with the capping unit mesas are distributed widely in all landing ellipse options.
- Like all the sites, Aram Dorsum performs less well at the 2 m baseline. At this length scale there is more geomorphic variation in the landing site, so areas that do not meet this criterion include those that fail the 7 m and longer baselines, as well as discontinuous contributions from the edges of the Aram Dorsum main inverted channel.
- Aram Dorsum dose not compare as well to Oxia Planum at 2 m baseline (54% of 1x1 km samples having <5% violation at Aram Dorsum compared to 70% at Oxia Planum) but is better than Mawrth Vallis (36%).
- It should be noted that this baseline is close to the resolution of the DTMs, so differences in image quality and pixel matching during DTM production might have influenced these results.
- Furthermore, whilst a good fit to these short baseline criteria is favourable from an engineering perspective, a lack of geomorphic features in the landing zone will negatively impact the performance of the Rover in completing the science objective: ExoMars Rover relies on standoff imaging instruments for geological characterisation before choosing drill sites. For geological characterisation to be possible, sufficient outcrops are required for the rover to investigate. In this respect Oxia Planum performs poorly, as it has few upstanding outcrops in the central areas of the ellipse (other than hazardous small craters) whereas Aram dorsum performs well will minimal small craters but several shallow pits and channel edges with geomorphology suitable for characterisation with the ExoMars Rover instrument suite.

2.3 CRATER DENSITY AND DISTRIBUTION

Impact craters can be landing hazards or impediments to Rover traversability. Their density can indicate formation and exposure age of a surface. Aram Dorsum Crater distribution is shown in Figure 16 – maps for the other sites are included in the appendix and summarised in Table 4.

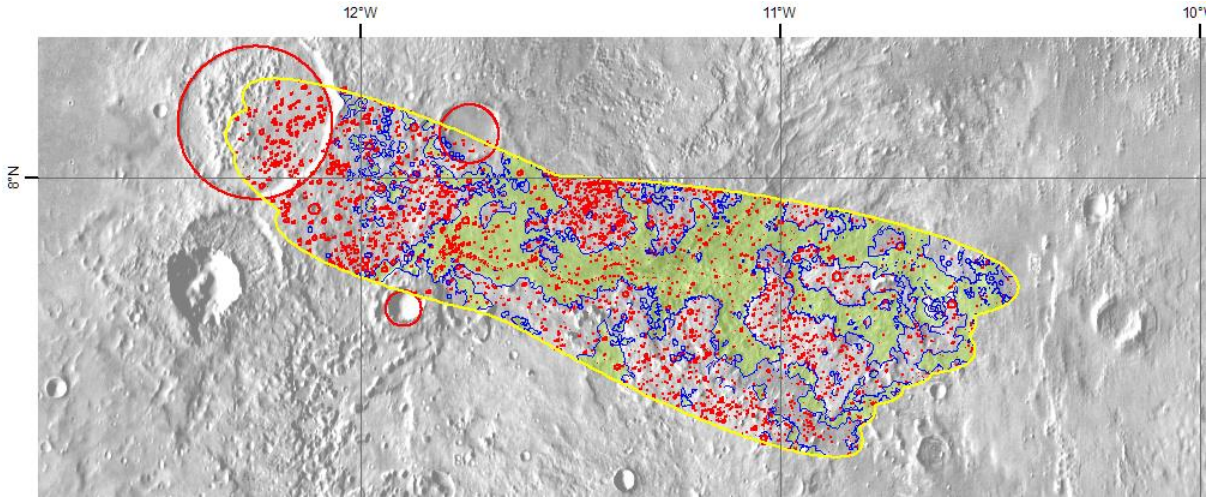

Fig. 16. *The distribution of impact craters across the Aram Dorsum landing ellipse pattern (yellow) showing impact craters (red) in areas of highest priority science targets (shaded green) and low priority areas (other). All craters are included for the purpose of understanding landing and traversability hazards. These data are not suitable for dating specific geological units. Crater counted using CTX base layer.*

Table 4. *Impact crater summary table for all sites. Sites have been split into "high science priority areas" and "non-priority areas".*

Landing site	*% ellipse pattern sampled*	*Craters per k^{-2}*	*Craters per km^2 (priority area)*	*Craters per km^2 (non-priority area)*
Aram Dorsum	*100%*	*1.56*	*0.96*	*1.93*
Mawrth Vallis	*58%*	*1.94*	*1.15*	*2.91*
Oxia Planum	*58%*	*3.78*	*3.73*	*4.17*

The spatial density and distribution of impact craters show spatial variation for Aram Dorsum and Mawrth Vallis. In both landing sites stratigraphically younger and darker materials have higher density of craters, whilst the older and brighter regions have relatively lower densities of craters. **Importantly, the low density areas are towards the centre of the Aram Dorsum ellipse and are areas of highest priority science targets**. In contrast, in Oxia Planum there is a greater density of impact crater morphologies distributed across the whole of the sampled area (see Appendix).

These results show that Aram Dorsum and Mawrth Vallis have younger surface exposure ages in the areas of high priority science targets than Oxia Planum. **Thus Aram Dorsum and Mawrth Vallis minimise outcrop exposure time in the Martian radiation environment and maximise probability of biosignature preservation.**

2.4 ALBEDO, THERMAL INERTIA, DUST

2.4.1 Albedo and thermal inertia

Our revised 2020 ellipses make no changes to the original compliance values (presented at first Landing Site Workshop) with regard to albedo and thermal inertia. Aram Dorsum is compliant.

2.4.2 Dust

We have compared Aram Dorsum dust cover with other lander and Rover sites using both TES and OMEGA data (Fig. 17). In TES data, Aram Dorsum has the lowest dust cover index value of any of the ExoMars candidate sites, and the majority of previous landing sites. However, due to the low resolution of the data, we need to consider OMEGA data.

In OMEGA data, Aram Dorsum has a lower dust cover than Viking 1 and Phoenix - which was also a solar-powered mission. It is also obvious at Aram, due to the low standard deviation, that the centre of the ellipse is representative of the rest of the ellipse areas. Oxia Planum has dust cover that is about the same as at the Pathfinder, Spirit and Opportunity landing sites. Mawrth Valles has a slightly lower dust cover index value than Oxia, but with the widest range across the ellipses (with maximum as high as values at Aram). Therefore, for Mawrth Vallis, the centre of the ellipse is not representative of the dust cover in the rest of the ellipse space, and dust cover should be considered to vary significantly.

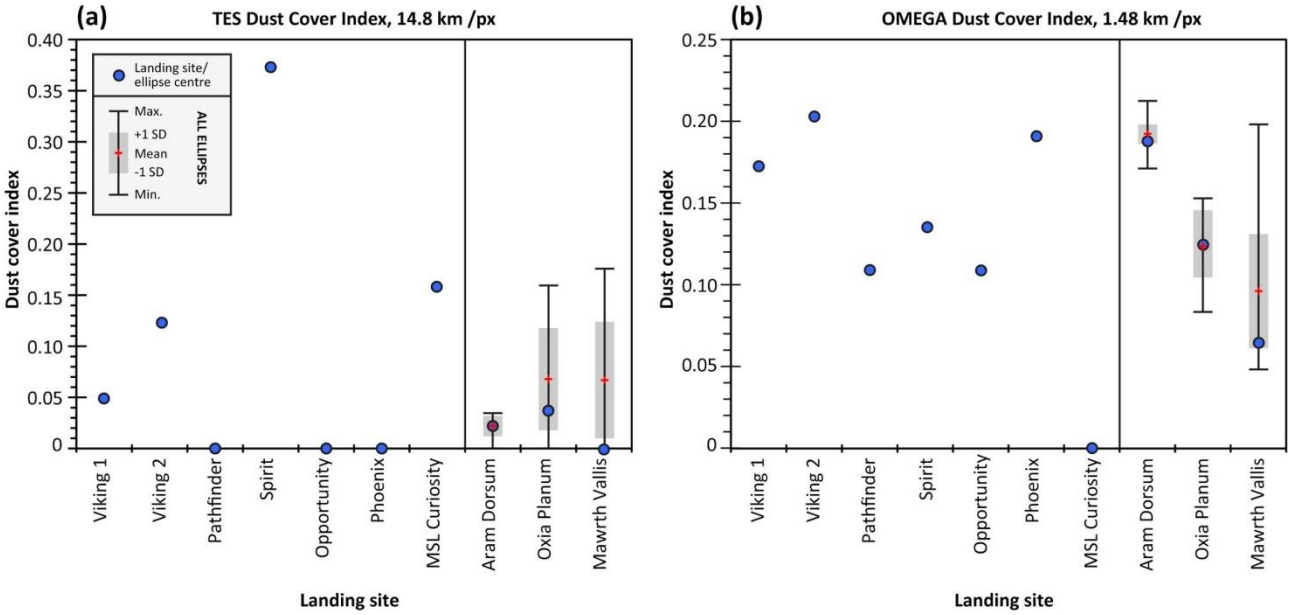

Fig. 17. *Dust analysis at Aram Dorsum, compared to other landing sites. (a) TES dust cover index values (14.8 km/pixel). (b) OMEGA dust cover index values (1.48 km/pixel).*

Dust Cover Summary

We know that Western Arabia Terra has a thin (likely minimum order of microns to tens of microns) veneer of dust, which often obscures orbital hyperspectral surveying. Nevertheless, the OMEGA dust cover index (1.5 km/px resolution) at Aram Dorsum is lower than or similar to other successful solar-powered mission landing sites (e.g. Phoenix) so this amount of dust should not be a problem for the mission.

2.5 ROCK ABUNDANCE

Our revised 2020 ellipses make no changes to the rock abundance results given by the LSSWG (our group helped produce the data for this).

2.6 OTHER ISSUES

2.6.1 Transverse Aeolian Ridges (Aeolian bedform cover)

We (with interns supervised by LSSWG member Bridges) have mapped decametre-scale aeolian bedforms ("Transverse Aeolian Ridges" or TARs[23]) across all three sites. There are no large "dark dune-type" bedforms in Aram Dorsum. Areas of TARs of similar density were mapped and digitised following the definitions of [23]). Test sites mapped both by Balme and the LSSWG interns were used to produce more consistent results, with data finally summarised in a "gridded" form. The appendix includes data for all three sites, with two sizes of gridding used to check for sampling issues. Mapping and summary results for Aram Dorsum are shown in Figure 18. Site comparison summary data are in table 5; only 1 km grids are considered here for simplicity (there is very little

difference in the outcomes from the two methods). Data and maps for other sites are shown in the appendix.

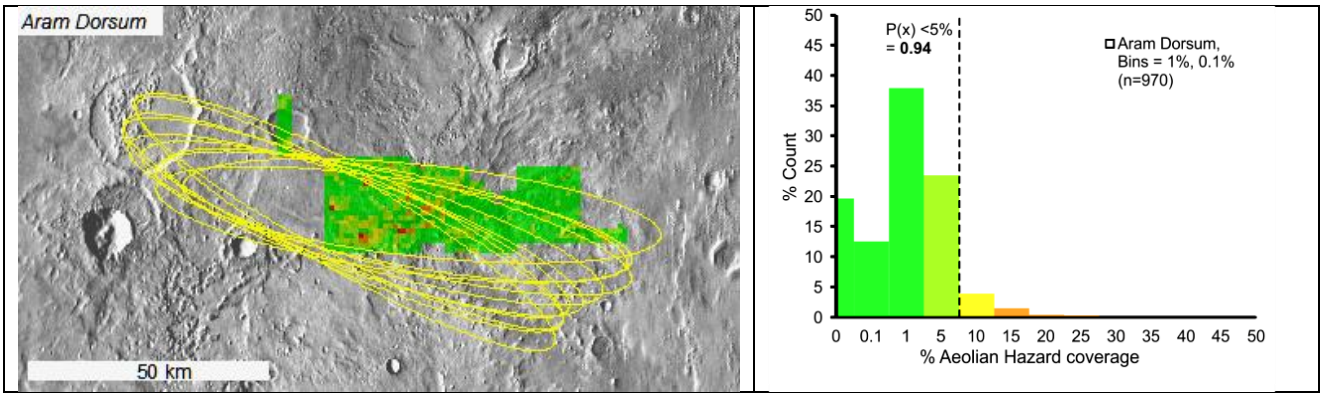

Fig. 18. *Aeolian TAR data for Aram Dorsum. Only the eastern part of the ellipse pattern has been mapped so far. Map colours indicate average areas of each cell covered by TARS. Green is lowest coverage, <5%, yellow is <10%, orange is <20% and red >20%. The same data are shown in histogram-form on the right (note that there are too few "red" areas to show in the histogram).*

Table 5. *Comparison of TAR cover for all three sites.*

Site	*Mean (%)*	*Max (%)*	*Min (%)*	*Stan dev.(%)*	*P(x) > 0.95*	*N*
Aram Dorsum	*1.35*	*41.0*	*0.0*	*3.0*	*0.94*	*970*
Mawrth Vallis	*11.1*	*69.1*	*0.0*	*10.4*	*0.34*	*449*
Oxia Planum	*4.3*	*53.5*	*0.0*	*6.6*	*0.77*	*1794*

Aeolian bedform cover summary

- Aram Dorsum has **the lowest cover** by aeolian bedforms of all three sites. The overall percentage cover is a mean of 1.35% with very few areas being above 20%.
- Aeolian bedforms are primarily located in impact craters in Aram Dorsum – areas to be avoided anyway as they present slope hazards. The floors of impact craters are often covered by aeolian bedforms in the other two sites as well.
- Oxia Planum generally has low aeolian bedform cover (~ 4.3%) except in the **centre/east** of the ellipse patterns where there are **extensive, fields of dense TARs and sub-TAR scale bedforms**. Even the sub-TAR scale landforms are likely to be ~ tens of cm tall. As this is slightly downrange of centre, these bedforms could be a significant hazard.
- The areas studied in Mawrth show a generally **very high** cover by aeolian landforms (11.1%) with significant areas of higher cover (numerous areas have 30-40% aeolian cover). Also, these areas appear to be distributed across the ellipse pattern, rather than being in a discrete location as is the case for Oxia Planum.

2.6.2 Comments on LSSWG loose deposits study.

We feel that this study has a number of weaknesses that mean that its conclusions – specifically the inference of *dust* lying in deposits tens of centimetres thick at all sites – are not robust.

1. The study only examines very small areas, so is not representative. Based on the size/number of the study areas, the following amounts of the respective ellipses are actually covered:
   a) Oxia. "Good quality images" = 0.13% of ellipse. All images = 0.15%

b) Mawrth. “Good quality images” = 0.11% of ellipse. All images = 0.13%

c) Aram. “Good quality images” = 0.12% of ellipse. All images = 0.15%

The study reports on much less than a fifth of one percent of the landing sites areas. Compare this with the TAR mapping where this number is from ~ 10% to over 50% of the study areas.

2. It is not possible to determine the size of objects smaller than 1-2 HiRISE pixel (~25-50 cm) using any Mars remote sensing data. There is no way to differentiate between flat lying areas of cobbles, coarse gravels, sand, silt or ‘dust’ in HiRISE. Sand-grade material can be identified by the presence of fresh-looking aeolian bedforms, but it is not possible to make detailed inferences about whether “smooth” areas are sandy, cobbled, competent, loose etc. We feel that an assumption of “featureless at HiRISE resolution = dust” has been made. This assumption is poor, as can be seen by examining data from other mission sites (e.g. Phoenix, MSL, MER) where small rocks and pebbles and apparently competent soils can be seen in-situ in areas that are apparently flat and featureless in HiRISE.

3. The idea that 75% of Aram’s surface is covered by “a dust cover from few cm to few 10s cm where the surface conditions and trafficability are uncertain” does not match our in-depth observations. There is little evidence to support this conclusion, and plenty to refute it (crisp crater morphologies, presence of ripples/TARs, visible fractures, visible float rocks etc.) E.g. Fig. 19.

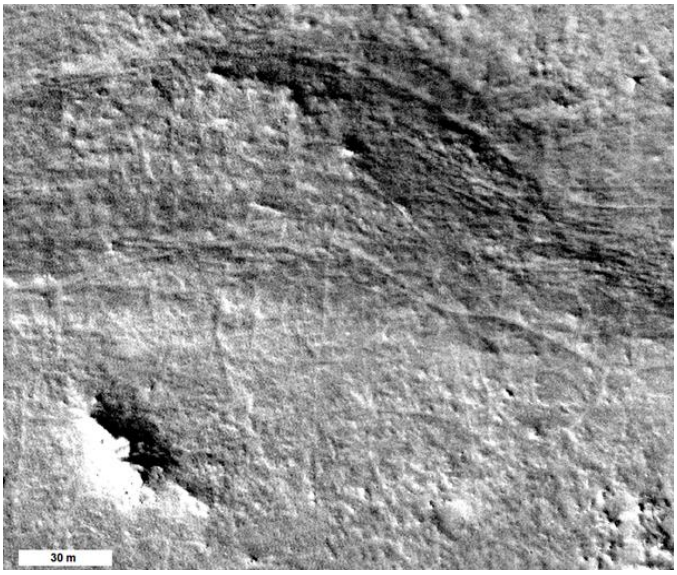

Fig. 19. *Example of typical surface detail in HiRISE in Aram Dorsum. Surface texture and structure, probably “bedrock” based on the fractures, suggest that if dust is present, it is certainly not at the “tens of cm scale”. Presence of float rocks, fractures, outcrop and albedo variations argue against significant dust cover.*

4. Contrasts in THEMIS nighttime images between different parts of the Aram Dorsum site can be clearly seen. This would not be the case if the surface was covered in tens of cm of dust. Similarly, a lack of difference in colour images does not mean that there is tens of cm thick dust. The dust cover could be very thin – perhaps just a few tens of microns.

5. The examples about depth of ‘dust’ deposits based on smooth looking craters are misleading. Many examples shown are not pristine craters: they have been heavily eroded (almost completely in many cases) before being filled with sediment. In fact, some of the craters have probably been infilled (possibly completely) by sedimentary material which has then been lithified (these could be drill targets if the fill was fluvial), and then undergone erosion – perhaps in many cycles. The whole of Aram Dorsum has probably been buried, lithified, then exhumed.

6. Not all bedrock will appear Mawrth-like with high albedo and obvious fracture patterns. Much of the Aram channel and channel marginal areas are probably bedrock of some kind (likely fine-grained sedimentary rocks). This is borne out by the THEMIS nighttime observations which show the channel marginal materials (one of the largest units in the map, and a prime science target) to be relatively bright (i.e., more consolidated).

3. SUMMARY TABLE, BASED ON OUR OBSERVATIONS AND MEASUREMENTS

Property	**Aram Dorsum**	**Mawrth Vallis**	**Oxia Planum**
Age span (Ga)	Older than Late Noachian	Early Noachian to early Hesperian	Middle to late Noachian (clays). Hesperian (delta)
General nature of aqueous sediments	Detrital (alluvial), multiple episodes	Mainly pedogenic & local fluvial clays. Clay variety	Pedogenic/detrital. Less clay variety than Mawrth
Duration of aqueous events	Unknown, potentially >3.9 – 3.5 Ga (>400 Ma)	Various events over 400 Ma	Various events over 400 Ma
What are the most interesting targets (their age in Ga)?	Extensive exhumed floodplains aged > 3.7 Ga	Clay units >3.6 Ga	Clay units, Unknown age probably >3.7 Ga sediment fan <3.7Ga
How much of ellipse has interesting targets?	~75%	48%	~85%
Are interesting targets small and far apart? Or distributed all over?	Extensive areas in centre of ellipse, possible inliers exposed in pits throughout ellipse	58% capping unit 48% potential target	Well distributed
Rock and mineral variety over short distances	Yes. Variety of geological units in ellipse, plus regional diversity from large fluvial catchment	No. One target lithology/environment with low priority capping unit overlain	Short distances yes, medium distance yes Most of the ellipse is one lithology; other lithologies present but hazardous
What is not high priority targets, is it interesting?	**Yes. Local overburden comprised impact-excavated materials, of potential interest**	**No. basaltic composition forming sand dunes**	**Yes, sediments fan, possible volcanic materials.**
Ponded water areas	yes	Don't know	yes
Signatures of possible low-T hydrothermal systems	Poss. sampled in catch-ment; deposited here	possible	Unlikely
Biosignature preservation: Fine grain size	Yes, on flood plains Coarser in channel belt resistant "cap" unit.	Sedimentary context unknown so no grain size estimate possible.	Yes, many layers, polygonal clays and also in delta fan
Biosignature preservation: Rapid burial	Yes	Unknown	Probable for clays Yes for delta fan
Biosignature preservation: Recent exhumation	Yes, better at foot of eroded buttes.	Yes. Most recent at foot of cap units	Yes. Most recent at foot of volcanic & delta units
Prime targets: Area coverage for 1, 3, 5-km traverse from centre	80%, 91%, 98%	92%, 95%, 100%	93%, 98%, 100%
EDL 2020	**Feasible-100 km**	**Feasible-120 km**	**Feasible-120 km**
Elevation: % of ellipse area below –2000 m MOLA	95.3%	94.3%	100%
Elevation: % of 99% (90%) ellipse below –2000 m MOLA	?	?	?
Slopes: % compliance 2–10 km	98.8	88.9	98.8
Slopes: % compliance at 330 m	98.9	98.5	99.2
Slopes: % compliance at 7 m	98.9	89.4	99.2
Slopes: % compliance at 2 m	94.2	90.6	95.7
Crater density:	1.55 craters per km^2	1.94 craters per km^2	3.78 craters per km^2
TAR coverage (% and where)	1.4% (per 2.5x2.5km)	10.8% (per 2.5x2.5km)	4.4% (per 2.5x2.5km)
Dust coverage (% and where)	Ellipse centre: 0.19 All ellipses: 0.19 ± 0.01 (0.17 – 0.21)	Ellipse centre: 0.08 All ellipses: 0.10 ± 0.04 (0.05 – 0.20)	Ellipse centre: 0.12 All ellipses: 0.13 ± 0.02 (0.08 – 0.15)
Thermal inertia: % area > 150	99% ≥ 150 $Jm^{-2}s^{-0.5}K^{-1}$	99.5% ≥ 150 $Jm^{-2}s^{-0.5}K^{-1}$	100% ≥ 150 $Jm^{-2}s^{-0.5}K^{-1}$
Albedo: % area in range 0.10–0.26	100% 0.1 – 0.26	100% 0.1 – 0.26	100% 0.1 – 0.26
Rock cover: No. of rocks size 1.50 m ≤ D ≤ 2.25 m			
Rock coverage: Fk (D) % fit for rocks with size D ≥ 35 cm			
Rock coverage: RAT results			
Planetary Protection	OK	OK	OK

4. REFERENCES

1. Davis, J.M., Balme, M., Grindrod, P.M., Williams, R.M.E., and Gupta, S. (2016), *Geology*, 44, 847-8506.
2. Hynek, B.M., Beach, M., and Hoke, M.R.T. (2010), *J. Geophys. Res.*, 115, E09008.
3. Hynek, B.M., and Di Achille, G. (2017), *U.S.G.S. Scientific Investigations* Map 3356, scale 1:2,000,000.
4. Wordsworth, R.D., Kerber, L., Pierrehumbert, R.T., Forget, F., and Head, J.W. (2015), *J. Geophys. Res.*, 120, 1201–1219.
5. Williams, R.M.E., Irwin, R.P., and Zimbelman, J.R. (2009), *Geomorph.*, 107, 300–315.
6. Tanaka, K.L., et al. (2014), *U.S.G.S. Scientific Investigations* Map 3292, scale 1:20,000,000.
7. Maizels, J.K. (1987), Desert Sediments: Ancient and Modern, *Geol. Soc. London, Sp. Pub.* 35, 31–50.
8. HaydenA.T., M.P. Lamb, W.W. Fischer, R.C. Ewing, B.J. McElroy (2017), *LPSC* XLVIII, abstract 2488.
9. Summons R.E., Amend J.P., Bish D., Buick R., Cody G.D., Des Marais D.J., Dromart G., Eigenbrode J.L., Knoll A.H., and Sumner D.Y. (2011), *Astrobiol.*, 11, 157–181.
10. Yen, A.S., S.S. Kim, M.H. Hecht, M.S. Frant, and B. Murray (2000), *Science*, 289, 1909-1912.
11. Irwin, R.P., Howard, A.D., Craddock, R.A., and Moore. J.M. (2005), *J. Geophys. Res.*, 110, E12S15.
12. Grotzinger, J.P., et al. (2014), *Science*, 343, 1242777.
13. Edgett, K.S., (2005), *Mars*, 1, 5-58.
14. Farley, K.A., et al. (2014), *Science*, 343, 1247166.
15. Johnson, J. R., P. R. Christensen, and P. G. Lucey (2002), *J. Geophys. Res.*, 107, E001405.
16. Carter, J.C., D. Loizeau, C. Quantin, F. Poulet, S. Gupta, J. Vago, and J.-P. Bibring (2015), EPSC2015-661.
17. Marzo, G. A., T. L. Roush, N. L. Lanza, P. C. McGuire, H. E. Newsom, A. M. Ollila, and S. M. Wiseman (2009), *Geophys. Res. Lett.*, 36, L11204
18. Noe Dobrea, E. Z., et al. (2010), *J. Geophys. Res.*, 115, E00D19,
19. Vaniman, D.T., et al. (2013), *Science*, 343, 1243480.
20. Milliken, R.E., J.P. Grotzinger, and B.J. Thomson (2010), *Geophys. Res. Lett.*, 37, L04201
21. Seelos, K.D., F.P. Seelos, C.E. Viviano-Beck, S.L. Murchie, R.E. Arvidson, B.L. Ehlmann, and A.A. Fraeman (2014), *Geophys. Res. Lett.*, 41, 4880–4887.
22. http://exploration.esa.int/mars/53462-call-for-exomars-2018-landing-site-selection/
23. Balme, M., Berman, D.C., Bourke, M.C., and Zimbleman, J.R. (2008), *Geomorph.*, 101, 703-720.

Appendix to 2020 ExoMars Rover landing site checklist: Aram Dorsum
P. Fawdon., M. Balme., P.M. Grindrod., J. Bridges, J.M. Davis, S. Gupta,
17th March 2017

Note: *This Appendix supports the report. This document presents data collected for all three ExoMars candidate landing sites. The purpose of this appendix to enable like-for-like comparison between these sites and to present the data we collected.*

1. BACKGROUND

1.1 Slope map methods

We have produced slope maps for the range of baselines originally detailed in the 2013 call for landing site proposals[1]. Slope calculations are performed in ArcMap 10.3 using two different slope calculations methods.

The first method is the average maximum technique[2] used in the ArcGis10.3 'slope tool' (hereafter referred to as; 'sl'). This tool performs slope calculation on a 3x3 moving window[3] and thus considers data over a baseline of 2 or 2.82 x the input raster call size. Data baselines and cell sizes are detailed in Table 2.

The second method, as recommended and described by ESA[4,5], is an adirectional slope method (Maximum Adirectional Slope method hereafter to as; 'mas'). This is given by the absolute value of the maximum slope computed around a point, measured at a specific length scale (e.g. the baseline lengths). This method has been adapted to the ArcGIS Python environment by calculating the tangent between elevation of a point and the maximum difference in elevation extracted from an annulus 1 cell in width at a mean distance of the baseline length from the point (processing script is available on request). No resampling of the data is required to perform this calculation. Results from this adaptation have been verified within the LSSWG.

1.2. Data availability

To calculate slopes we have used the data sets given in Table 1. The sampling strategy and how representative the data are of the terrain at the three landing sites is discussed in the relevant section. Figure 1 shows the distribution of elevation and long baselines hazards for each landing ellipse pattern. Also shown is the total coverage of HiRISE DTM data.

Three approaches have been taken to sample the data. For elevation and long baseline slopes (where data coverage captures the majority of the landing ellipse patterns) we have sampled 10 ellipses at a range of azimuths between the maximum and minimum provided by the LSSGW. This approach has been taken to explore the full range of potential azimuths within the launch window. For short baseline data (i.e. evaluated using HiRISE DTM's) we initially sampled 'per DTM', however this was not found to sufficiently explore the distribution of the data. Therefore, we have additionally sampled the HiRISE data through a 1x1 km grid, permitting a thorough exploration of the areas of good and bad slopes.

2. DATA

2.1 Elevation and Slope hazards overview

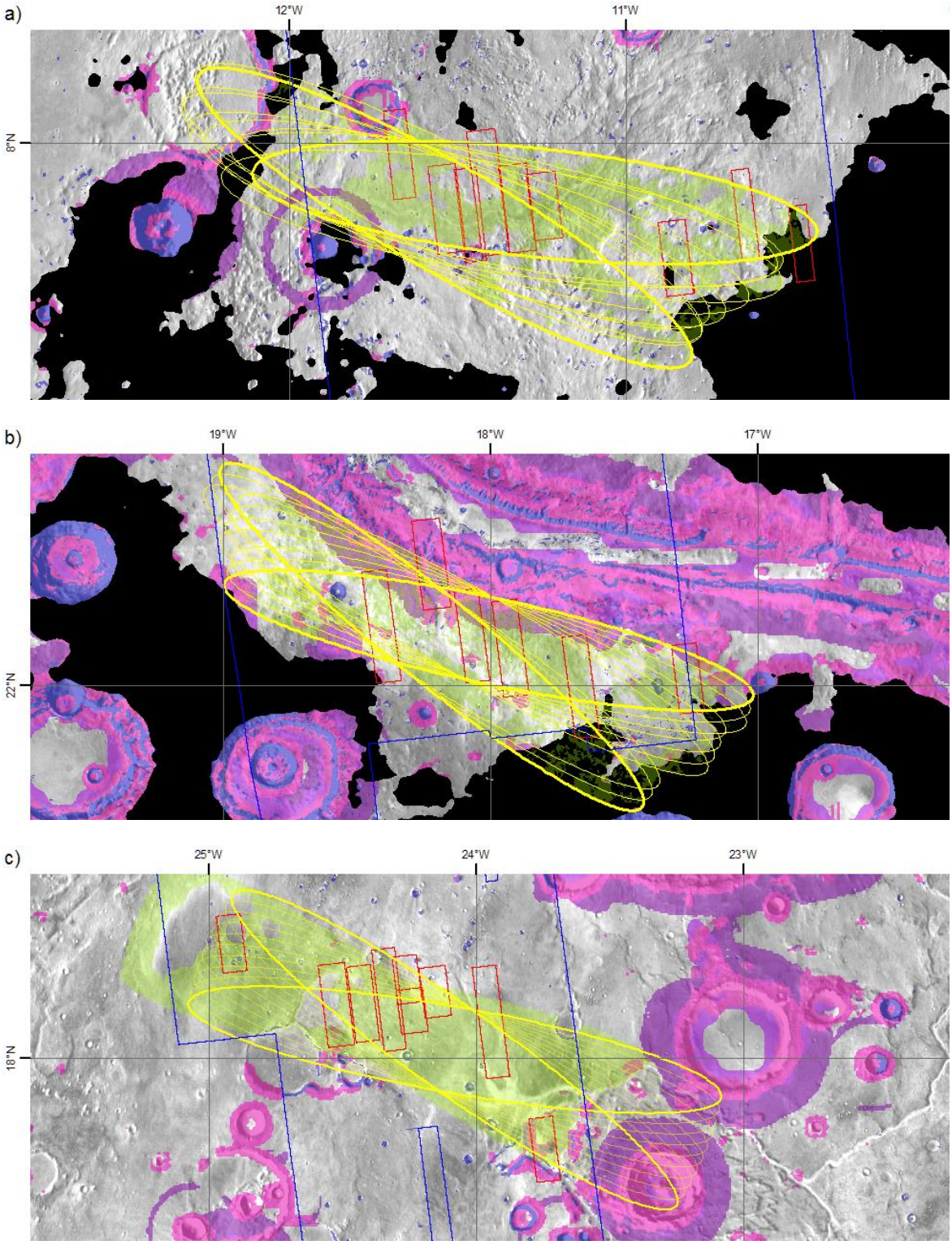

Fig. 1. *Elevation and Long baseline slope hazards at the (a) Aram Dorusm, (b) Mawrth Vallis and (c) Oxia Planum landing sites. Areas outside the -2000m elevation criterion are shaded* ***black****. Slopes calculated by both methods are coloured by baseline: 10 km in* ***purple****, 2 km in* ***pink*** *and 330 m in* ***blue****. The thick yellow ellipses show the maximum and minimum azimuth ellipses and the lighter yellow ellipses denote the 10 sample azimuths used to evaluate the elevation and long baseline slope hazards. Also shown is the coverage of HiRISE DTM's in red, and CTX DEM coverage in blue outlines. An estimation of the high priority 'land on' science targets'; shaded green.*

Table 1. *Data baselines and coverage at candidate sites*

Critera	Data	Method/Cell size	Rationale	AD	MV%	OP
-2000m elevation	MOLA Points			100%	100%	100%
	MOLA Gridded			100%	100%	100%
	HRSC DTM			100%	100%	0%
10 km (2˚)	MOLA points	_sl (Gridded to 3333 m)	To ensure slant and incidence is compatible with radar	100%	100%	100%
	MOLA Gridded	_mas				
2 km (3˚)	MOLA points	_sl (gridded to 666 m)		100%	100%	100%
	MOLA Gridded	_mas				
330 m (8.6˚)	HRSC MC11E DA5	_sl (re-gridded to 110 m)	To ensure proper fuel consumption during powered decent	100%	100%	0%
	HRSC MC11E DA5	_mas				
	CTX DTM's	_sl (regridded to 110 m)		85%	82%?	83%%
	CTX DTM's	_mas				
7 m (12.5˚)	HiRISE DTM's	_sl (regridded to 2.3 m)	To ensure adequate altitude error at touch down	21%	16%	17%
	HiRISE DTM's	_mas				
2 m (15˚)	HiRISE DTM's	_sl (regridded to 2.3 m)	To ensure stability at landing	21%	16%	17%
	HiRISE DTM's	_mas				

2.2 Elevation data

We used HRSC and MOLA data to compare the elevation constraint (terrain must be < -2000 m) for the three sites. To fully characterise these parameters, we sampled ellipses with 10 azimuths across the range expected during the 2020 launch window. We used a range of ellipse centre points to minimise violations of these engineering criteria and maximise landing on the highest priority science targets. Ellipse centre points were obtained from the various site proposing teams. Fig 2 summarises the elevation criterion results for all three sites.

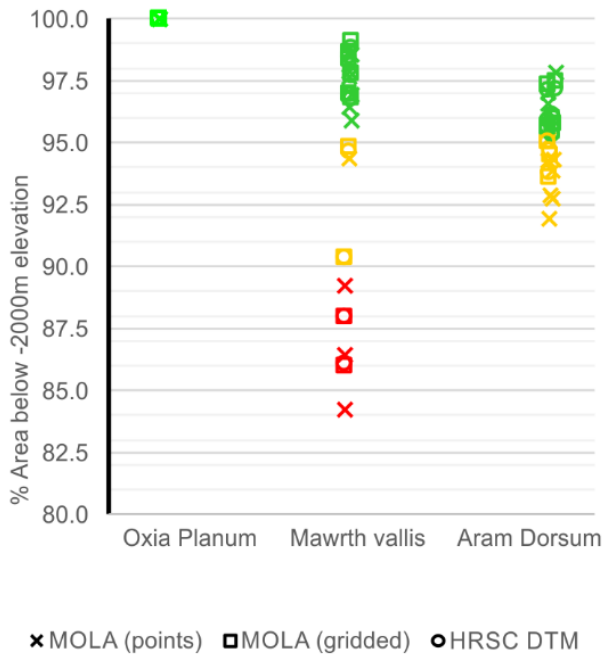

Fig. 2. *The percentage area below the -2000m elevation criteria for the 10 sample azimuths at each of the proposed landing sites*

Landing site	*Mean (%)*	*Max (%)*	*Min (%)*	*Standard deviation*
Aram Dorsum	*95.3*	*97.8*	*91.9*	*1.5*
Mawrth Vallis	*94.3*	*99.1*	*84.2*	*4.8*
Oxia Planum	*100.0*	*100.0*	*100.0*	*0.0*

2.2.1 Data reliability, representativeness and fit to the -2000m elevation constraints

MOLA gridded and point data provide complete coverage of all the landing sites, and HRSC data is also available for Aram Dorsum and Mawrth Vallis. These results are representative of the chosen ellipse patterns, showing that all of Oxia Planum meets the criteria, whereas Aram Dorsum and Mawrth Vallis have a mean compatibility of ~ 95%, however the area above -2000 m is restricted to the extreme ends of the ellipse pattern. This problem can be ameliorated for Mawrth by moving the ellipses to an alternative "Backup" higher azimuth position, which brings all samples to <10% failure of the elevation criteria, but at a cost to the 2-10 km baseline slope criteria and access to targets (see Fig. 1).

2.3 Slopes

2.3.1 Long Baseline Slopes

Slopes over long baselines (2 – 10 km and 330 m) are important to ensure that slant and incidence are compatible with the radar system and that there is proper fuel consumption during powered descent. To fully characterise these slopes, again we sample ellipses with 10 azimuths throughout the range expected during the 2020 launch window. Long baseline statistics for 10 sample azimuths at all landing sites are shown in Fig. 3.

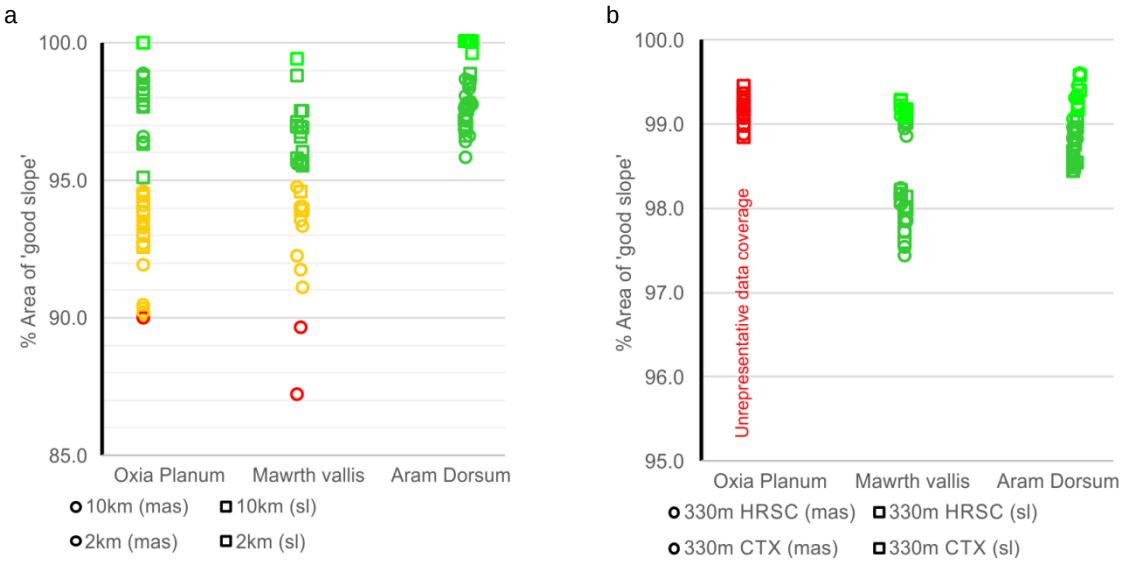

Fig. 3*. The percentage of 'good' slope area for (a) slopes over 10 km and 2 km (<2˚ and <3˚) baselines and (b) slopes < 8.6˚ over a 330 m baseline for 10 azimuths summing result from both the 'sl' and 'mas' method, and for both HRSC and CTX data for the 330 m baseline. Note that due to lack of CTX DEM cover for Oxia Planum, and the fact that the ellipses overlap significant slope hazards to the east (~ 10 km diameter craters), the 330m baseline data are not considered representative: it is likely that more of the ellipse areas will fail the criterion than displayed here.*

Baseline/Landing site	***Mean (%)***	***Max (%)***	***Min (%)***	***Standard deviation***
Baseline 10 km (2˚)				
Aram Dorsum	*98.8*	*100.0*	*96.6*	*1.3*
Mawrth Vallis	*88.9*	*99.4*	*76.1*	*8.3*
Oxia Planum	*91.8*	*100.0*	*89.9*	*3.6*
Baseline 2 km (3˚)				
Aram Dorsum	*97.6*	*100.0*	*95.8*	*1.1*
Mawrth Vallis	*94.6*	*97.1*	*89.6*	*2.1*
Oxia Planum	*96.0*	*98.9*	*92.5*	*2.4*
Baseline 330 m (8.6˚)				
Aram Dorsum	*98.9*	*99.6*	*98.4*	*0.4*
Mawrth Vallis	*98.5*	*99.3*	*97.4*	*0.6*
Oxia Planum	*99.1*	*99.4*	*98.8*	*0.2*

2.3.2 Data reliability, representativeness and fit to slopes over the 2-10 km baseline

At Oxia Planum, the 3 sigma ellipse pattern only exceeds the 2-10 km slope baseline in association with an impact crater at the east end of the ellipse pattern. The 330 m baseline is probably also exceeded here, but this area is outside the DTM coverage (thus the result here is a minimum). Elsewhere, scarps sporadically exceed the 330 m constraint. At Aram Dorsum there is minor infringement of the long baseline associated with a scarp in the far west and an impact crater to the south. Infringement at the 330 m baseline also occurs here and at a group of small mesas, again in the south. At Mawrth Vallis the 10 km and 2 km constraints are exceeded throughout the north of the ellipse pattern and these results become worse when employing the "Backup" higher azimuth ellipse positons which give better elevation constraint agreement. The violations at the 330 m baseline occur throughout the ellipse in association with scarps along the margins of the capping unit distributed throughout the landing ellipse.

2.3.3 Short Baseline Slopes (by DTM)

To evaluate slopes over short baselines (i.e. evaluated using HiRISE DTM data) we initially evaluated the data on a per DTM basis. This was done because DTM coverage is generally in the centre of the ellipse (Fig. 11) and so is representative for all azimuths. Short baseline statistics for 10 sample azimuths at all landing sites are shown in Fig. 4.

a) b)

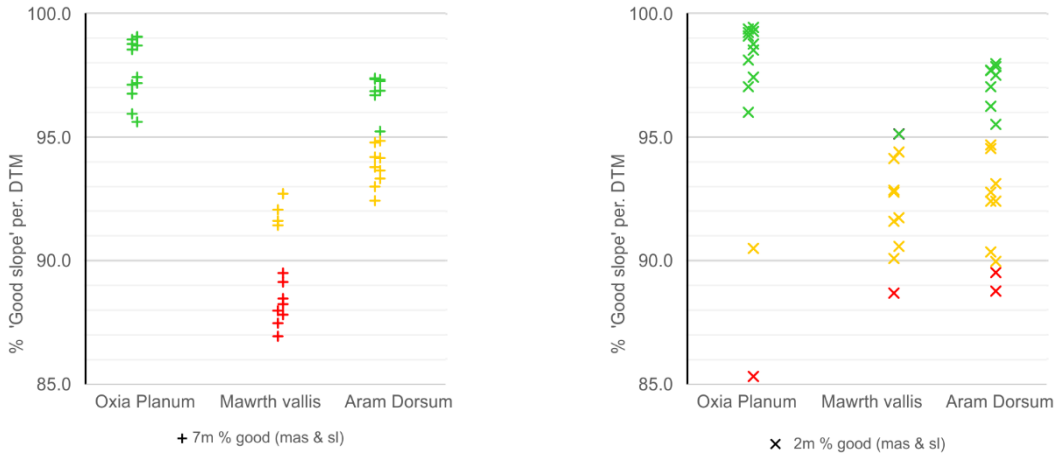

Fig. 4. *The percentage of 'good' pixels per HiRISE DTM for the (a) 7 m (12.5˚) and 2 m (15˚) baselines for DTM's in each of the three landing ellipse patterns. The results fold together both the sl and mas method. DTMs with poor quality data (e.g. Oxia 3 and 6) have been removed.*

Baseline/Landing site	Mean (%)	Max (%)	Min (%)	Standard deviation	no. DTM's sampled
Baseline 7 m (12.5˚)					
Aram Dorsum	95.4	97.2	92.4	1.7	16
Mawrth Vallis	89.4	92.7	87.0	2.0	12
Oxia Planum	95.4	89.9	80.6	5.9	14
Baseline 2 m (15˚)					
Aram Dorsum	94.2	97.9	88.8	3.0	16
Mawrth Vallis	90.6	95.1	82.2	4.1	12
Oxia Planum	95.7	98.9	83.3	5.4	14

2.3.4. Short Baseline Slopes (by 1x1 km samples)

Over short baselines (i.e. evaluated using HiRISE DTM data) we also used a grid of 1x1 km samples (Fig 5). This approach has been chosen because sampling by the full HiRISE DTM area poorly explores the distribution of slopes across the ellipse and does not cover the full ellipse area.

Aram Dorsum

a) *7m Baseline*

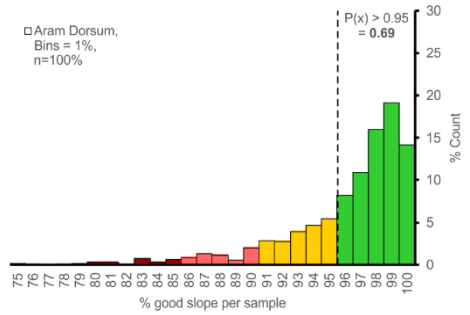

b) *2m Baseline*

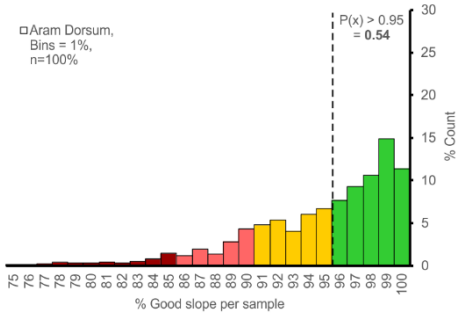

Baseline	*Mean*	*Max*	*Min*	*Standard devation*	*P(x) > 0.95*
7m (12.5˚)	*94.6*	*100.0*	*27.0*	*7.5*	*0.69*
2m (15˚)	*93.6*	*100.0*	*36.7*	*6.7*	*0.54*

Mawrth Vallis

c) *7m Baseline*

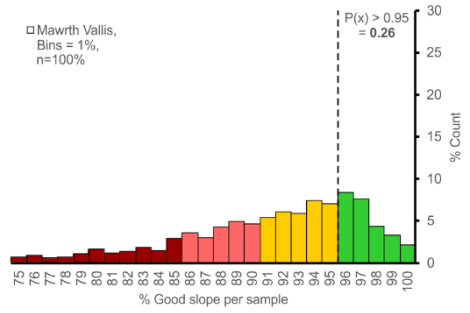

d) *2m Baseline*

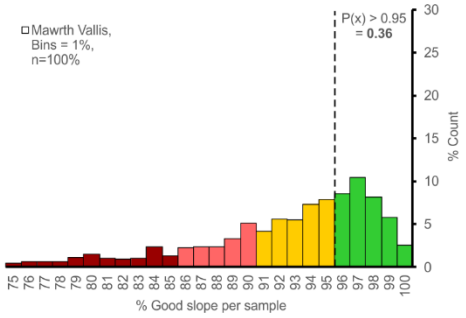

Baseline	*Mean*	*Max*	*Min*	*Standard devation*	*P(x) > 0.95*
7m (12.5˚)	*0.88*	*100.0*	*26.2*	*9.4*	*0.26*
2m (15˚)	*90.0*	*100.0*	*17.6*	*7.0*	*0.36*

Oxia Planum

e) *7m Baseline*

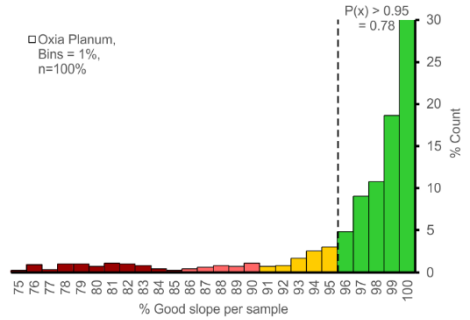

f) *2m Baseline*

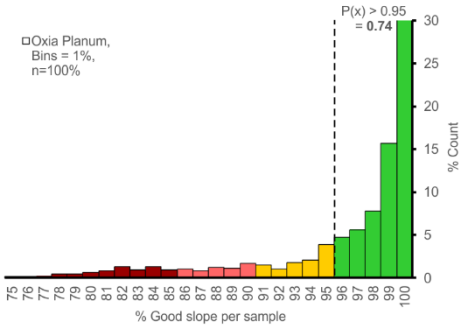

Baseline	*Mean*	*Max*	*Min*	*Standard devation*	*P(x) > 0.95*
7m (12.5˚)	*95.3*	*100.0*	*22.8*	*8.0*	*0.78*
2m (15˚)	*95.0*	*100.0*	*38.3*	*7.0*	*0.74*

Fig. 5. *These histograms summarise the percentage of each of the 1x1 km slope map samples that pass the slope criteria for a given baseline/threshold. Also marked is the probability that a 1x1km samples will have >95% area that pass the slope threshold for that baseline.*

2.3.5 Data reliability, representativeness and fit to slopes over the 2-7 m baseline

At the baseline lengths of 2 to 7 m (figures 4 and 5), violations are associated with small scarps and impact craters found across all landing sites. At Oxia Planum, violations are dominated by secondary impact crater chains that cross the ellipse. At Aram Dorsum, violations are caused by small scarps in the overburden units. At Mawrth Vallis, violations are distributed throughout the DTMs and are associated with scarps bounding the capping unit and some impact crater walls.

It is important to note that areas with Transverse Aeolian Ridges (TARs) and sand dunes also frequently exceed this criterion. However, these are areas of poor pixel matching in DTM production. Consequently, these results underestimate the hazard at this baseline when noisy areas of the DTM are removed or have yet to be sampled by a DTM.

Additionally, the size and position of DTMs are not random and so the "per DTM" data are not as representative as we would like. We have addressed this by sampling the DTMs with a 1x1 km grid. These results (Figure 5) better reflect the range and distribution of slope hazards on the 2-7 m baseline at the three landing sites. They also provide a probability of landing in a 1x1 km square with >95% 'good slope' pixels for each site.

2.4 Crater density and distribution

We have marked the location and diameters of all the impact craters across the sample areas in all the landing sites. We compare the variations in crater density in the ellipse and how this relates to different geological units, impact processes and the erosional history of the landing sites. Impact crater terrain distribution is shown in Fig. 6.

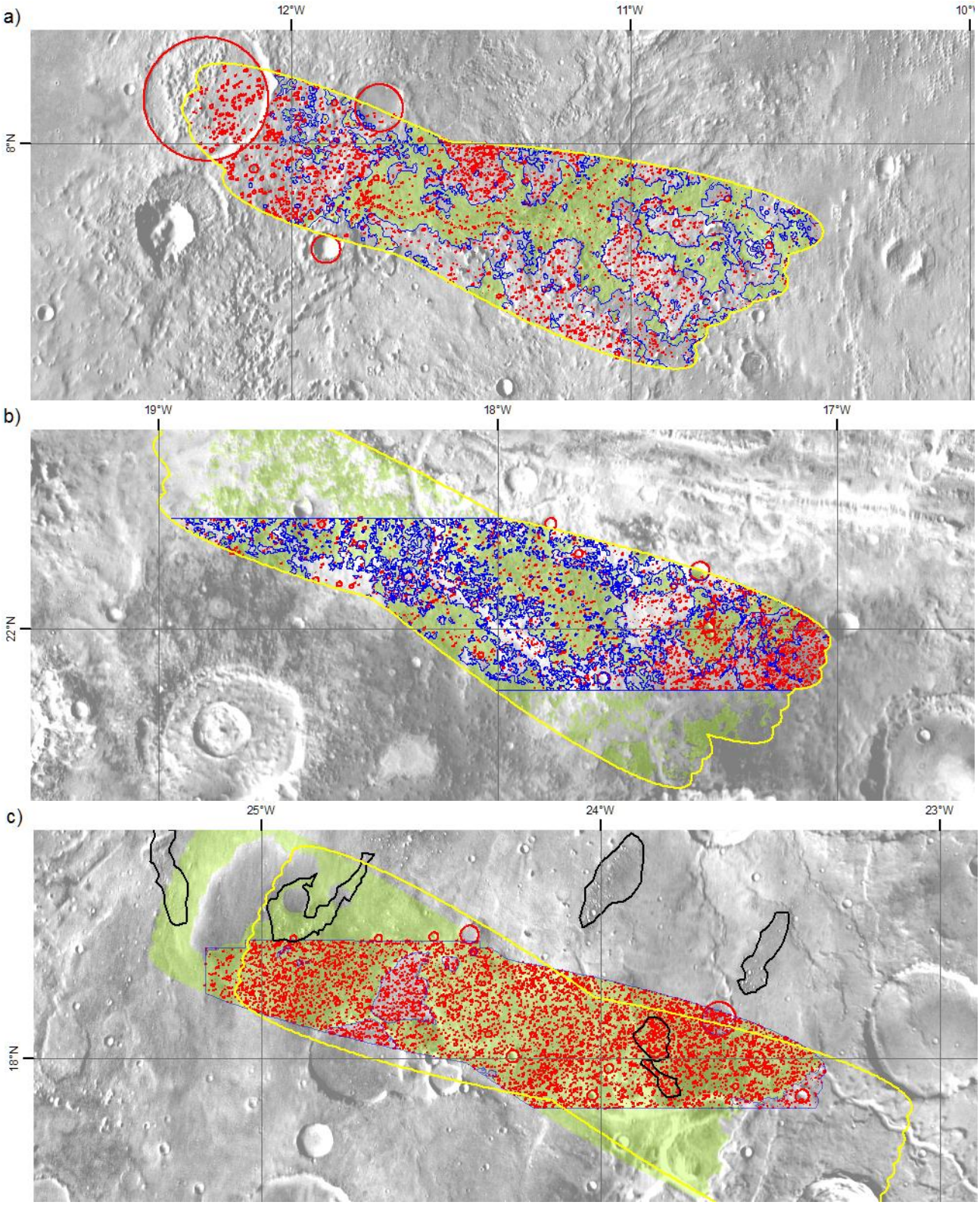

***Fig. 6**. The Distribution of impact craters (red circles) in the (a) Aram Dorsum (b) Mawrth Vallis and (c) Oxia Planum ellipse patterns divided by areas of high (green shading) and low priority (unshaded) science targets. All craters, included degraded craters, are included in these maps Craters have been counted on a CTX base layer at all sites. However, at Oxia Planum, craters have only been counted down to 50 m diameter. Also shown are areas of extremely dense secondary crater chains (black outlines).*

Landing site	***% ellipses sampled***	***no. km^{-2}***	***no. km^{-2} (target)***	***no.km^{-2} (not target)***
Aram Dorsum	*100%*	*1.56*	*0.96*	*1.93*
Mawrth Vallis	*58%*	*1.94*	*1.15*	*2.91*
Oxia Planum	*58%*	*3.78*	*3.73*	*4.17*

2.4.1 Impact crater data reliability, representativeness and results

The spatial density and distribution of impact morphologies show variation in cratering density at all the landing sites. At all sites, the areas of lower priority science targets have higher density of craters whilst areas of higher priority science target have lower densities of crater morphologies. In addition, areas of Oxia Planum have chains of secondary craters. These areas have the greatest density of impact crater morphologies and the terrain is totally dominated by impact crater morphologies (black outlines, figure 6).

The result indicate that Aram Dorsum and Mawrth Vallis have younger surface ages in the areas of high priority science targets indicating recent exposure relative to the ove burden materials at these landing sites. The density at Oxia Planum indicates lower erosion rates and thus the 'land on' surface has been exposed for longer. Therefore these results also indicate that Aram Dorsum and Mawrth Vallis (in particular their areas of high science priority) pose the least crater-related hazard to EDL and Rover traverses, whereas there is significant likelihood of encountering cratered terrain at Oxia Planum.

2.5 Transverse Aeolian Ridges

We (with interns supervised by LSSWG member Bridges) have mapped decametre-scale aeolian bedforms ("Transverse Aeolian Ridges" or TARs[6]) across all three sites. Areas of TARs of similar density were mapped and digitised following the definitions of [6]). Test sites mapped both by Balme and the LSSWG interns were used to produce more consistent results, with data finally summarised in a "gridded" form. The appendix includes data for all three sites, with two sizes of gridding used to check for sampling issues. Mapping and summary results for Aram Dorsum are shown in Figure 7.

Aram Dorsum

2.5 km x 2.5 km grid samples

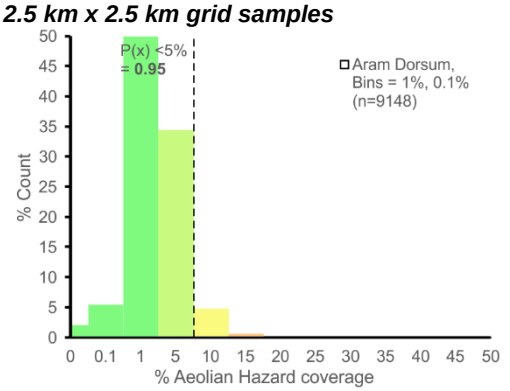

1 km x 1 km grid samples

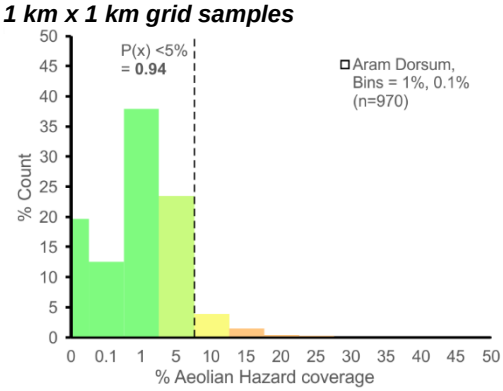

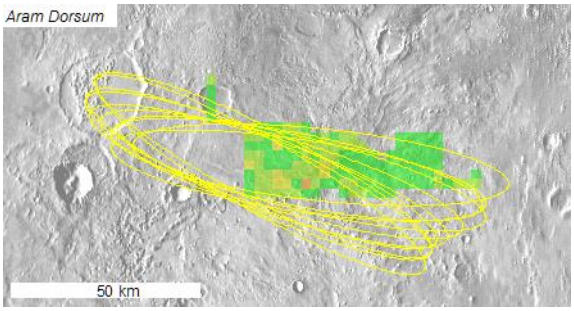

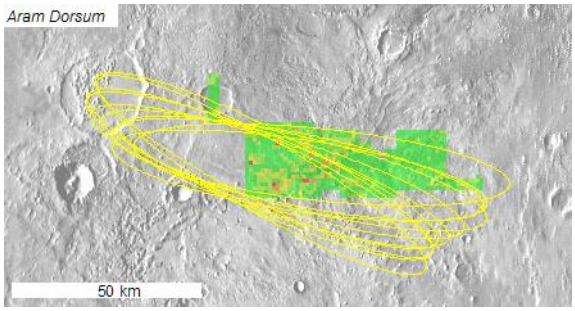

Sample size	*Mean (%)*	*Max (%)*	*Min (%)*	*Standerd dev.(%)*	*P(x) > 0.95*	*no. samples*
2.5x2.5 km	*1.4*	*13.5*	*0.0*	*1.9*	*0.95*	*148*
1x1 km	*1.4*	*41.0*	*0.0*	*3.0*	*0.94*	*970*

Mawrth Vallis

2.5 km x 2.5 km grid samples

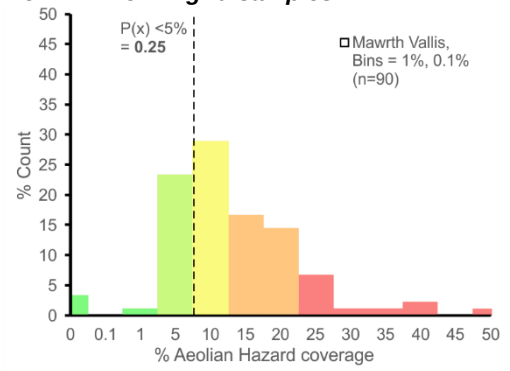

1 km x 1 km grid samples

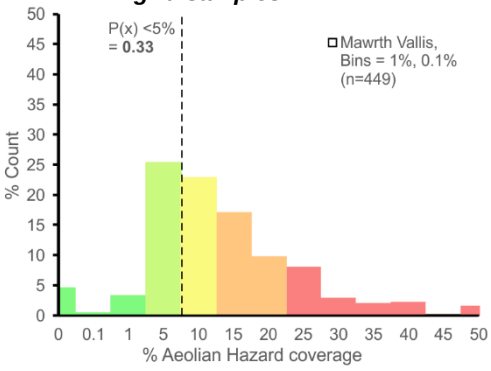

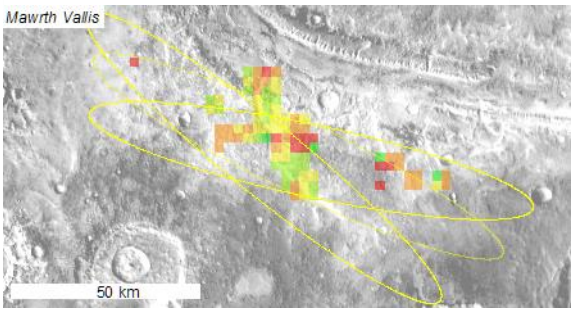

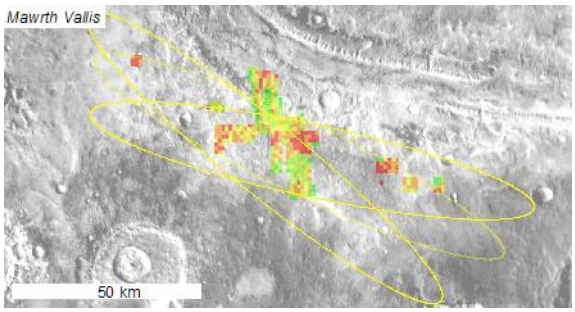

Sample size	*Mean (%)*	*Max (%)*	*Min (%)*	*Standerd dev.(%)*	*P(x) > 0.95*	*no. samples*
2.5x2.5 km	*10.8*	*50*	*0*	*8.9*	*0.27*	*90*
1x1 km	*11.1*	*69.1*	*38.3*	*10.4*	*0.34*	*449*

Oxia Planum

2.5 km x 2.5 km grid samples

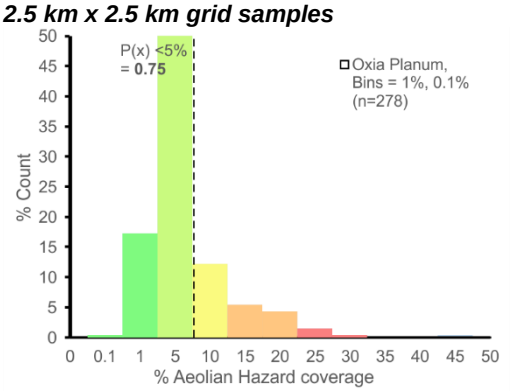

1 km x 1 km grid samples

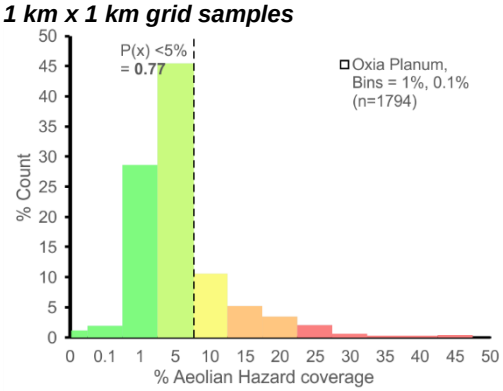

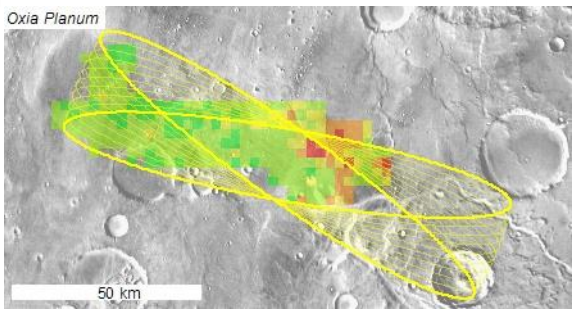

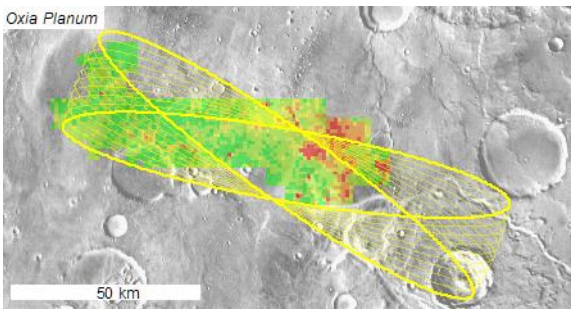

Sample size	*Mean (%)*	*Max (%)*	*Min (%)*	*Standerd dev.(%)*	*P(x) > 0.95*	*no. samples*
2.5x2.5 km	*4.4*	*42.5*	*0.1*	*5.3*	*0.76*	*278*
1x1 km	*4.3*	*53.5*	*0.0*	*6.6*	*0.77*	*1794*

Figure 7. *Aeolian Hazard at the three sites. Proportion of grid squares covered by TARs are shown for 2.5x2.5 km and 1x1 km samples. In both Map and hostrogram Green is lowest coverage, <5%, yellow is <10% ,orange is <20% and red > 20%.*

2.5.1 Data reliability, representativeness and results

The overall result is that Aram Dorsum has the smallest cover by aeolian bedforms (mean of 1.4%) compared with Oxia (mean 4.4%) and Mawrth (mean 11%). The two grid sizes give the same result. Oxia clearly has large areas with significant TAR coverage in the east/centre of the ellipse (and during our mapping we also identified vast quantities of sub-TAR scale bedforms in this region too), but otherwise only has high aeolian cover in local topographic traps (usually craters). If the mission “lands long” this areas could be a significant hazard to traversability. Aram has only small, widely distributed areas of high bedform cover, again mainly in craters. Mawrth, though, has large amounts of bedform cover associated with degrading capping and mesa units. These are large areas of hazard, and occur across the centre of the ellipse.

It should be noted, however, that most of the ellipse pattern has been covered in Oxia Planum, about 50% in Aram Dorsum, but far less mapping (~10-20%) has been done in Mawrth.

3. REFERENCES

1. http://exploration.esa.int/mars/53462-call-for-exomars-2018-landing-site-selection/
2. http://desktop.arcgis.com/en/arcmap/10.3/tools/spatial-analyst-toolbox/how-slope-works.htm
3. Burrough, P. A., and McDonell, R. A., 1998. Principles of Geographical Information Systems (Oxford University Press, New York), 190 pp.
4. EXM-MS-ANA-ESA-00001 ExoMars Rover Landing Site Slope Distribution Recommendation v1.0
5. FCXNL-11A06-2143067-1-2143067masarotto

1. 6. 23. Balme, M., Berman, D.C., Bourke, M.C., and Zimbleman, J.R. (2008), *Geomorph.*, 101, 703-720.